eTransportation 18 (2023) 100274

Contents lists available at ScienceDirect

eTransportation

journal homepage: www.journals.elsevier.com/etransportation

Lithium-ion battery utilization in various modes of e-transportation

Benedikt Tepe [a,*], Sammy Jablonski [a], Holger Hesse [b], Andreas Jossen [a]

[a] Chair of Electrical Energy Storage Technology, Department of Energy and Process Engineering, School of Engineering and Design, Technical University of Munich (TUM), Germany

[b] Kempten University of Applied Sciences, Department of Mechanical Engineering, Institute for Energy and Propulsion Technologies, Germany

ARTICLE INFO

Keywords:
Lithium-ion battery stress factors
Modes of transportation
Mobile applications
Electric cars
Electric buses
Electric boats

ABSTRACT

The electrification of the transportation sector leads to an increased deployment of lithium-ion batteries in vehicles. Today, traction batteries are installed, for example, in electric cars, electric buses, and electric boats. These use-cases place different demands on the battery. In this work, simulated data from 60 electric cars and field data from 82 electric buses and six electric boats from Germany are used to quantify a set of stress factors relevant to battery operation and life expectancy depending on the mode of transportation. For this purpose, the open-source tool *SimSES* designed initially to simulate battery operation in stationary applications is extended toward analyzing mobile applications. It now allows users to simulate electric vehicles while driving and charging. The analyses of the three means of transportation show that electric buses, for example, consume between 1 and 1.5 kWh/km and that consumption is lowest at ambient temperatures around 20 °C. Electric buses are confronted with 0.4–1 equivalent full cycle per day, whereas the analyzed set of car batteries experience less than 0.18 and electric boats between 0.026 and 0.3 equivalent full cycles per day. Other parameters analyzed include mean state-of-charges, mean charging rates, and mean trip cycle depths. Beyond these evaluations, the battery parameters of the transportation means are compared with those of three stationary applications. We reveal that stationary storage systems in home storage and balancing power applications generate similar numbers of equivalent full cycles as electric buses, which indicates that similar batteries could be used in these applications. Furthermore, we simulate the influence of different charging strategies and show their severe impact on battery degradation stress factors in e-transportation. To facilitate widespread and diverse usage, all profile and analysis data relevant to this work is provided as open data as part of this work.

1. Introduction

The market introduction of lithium-ion battery technology in the 1990s and its advancement since then is considered as enabler for the widespread electrification of the transportation sector [1]. Cars, buses, and boats are increasingly powered by electricity, replacing internal combustion engine-based propulsion systems [2–4]. Sales of electric cars (e-Cars) worldwide doubled to a total of 6.6 million from 2020 to 2021 [2]. In the same timeframe, sales of electric buses (e-Buses) increased by 40% worldwide, although the total number of buses remained constant [2]. For example, Hochbahn Hamburg, the operator of Hamburg's subways and buses, plans to electrify its entire bus fleet by 2030 [5]. The global market for electric boats (e-Boats) is also expected to double in volume from 2022 to 2028 [4]. These three modes of transportation vary in several aspects, such as average travel distance and frequency. In addition, vehicle usage also varies within a mode. For example, e-Buses typically travel longer distances than e-Cars, and e-Cars themselves may be used for daily commuting or just for leisure activities. Accordingly, the load on the battery system and the time available for charging the vehicles differs.

The present work analyzes the battery system load of different e-transportation modes. For this purpose, field data were collected from industry partners for the e-Buses and e-Boats. For e-Car data, a simulation tool is used, which is based on mobility data and simulates driving behavior. The collected data is used to emulate trips and charging behavior of the mobile applications with the help of *SimSES*, an open-source simulation tool extended for this purpose [6,53]. In an energy consumption analysis, the consumption of the vehicles is compared, and, for the e-Buses, the influence of the outside temperature is also shown. Various battery parameters such as the average state of charge (SOC), are then derived and compared. In addition, the parameters of the mobile battery storage systems (BSSs) are compared with those of stationary BSSs in three applications. We also consider the influence of

* Corresponding author. Electrical Energy Storage Technology, Technical University of Munich (TUM), Arcisstr. 21, 80333, Munich, Germany.
E-mail address: benedikt.tepe@tum.de (B. Tepe).

https://doi.org/10.1016/j.etran.2023.100274
Received 12 May 2023; Received in revised form 21 July 2023; Accepted 22 August 2023
Available online 23 August 2023

Nomenclature

Abbreviations

BSS	Battery storage system
e-Boat	Electric boat
e-Bus	Electric bus
e-Car	Electric car
EMS	Energy management system
EPA	Environmental Protection Agency
EV	Electric vehicle
eVTOL	Electric vertical take-off and landing
FCR	Frequency containment reserve
KPI	Key performance indicator
LMP	Lithium-metal-polymer battery
NEDC	New European Driving Cycle
NMC	Nickel-manganese-cobalt lithium-ion battery
PHEV	Plug-in hybrid electric vehicle
PV	Photovoltaic
PS	Peak-shaving
RQ	Research question
SCI	Self-consumption increase
V2G	Vehicle-to-grid
WLTC	Worldwide harmonized Light-duty vehicles Test Cycles

Parameters and variables

$b(t)$	Binary value indicating connection to electricity grid
C-rate	Charge rate
$C_{act}(t)$	Currently charged electrical charge
$C_{total}(t)$	Currently total possible capacity
$C_{\text{rate, abs}}(t)$	Currently absolute C-rate
$\text{Consumption}_{\text{trip}}$	Energy Consumption of a trip
$\Delta\text{SOE}_{\text{trip}}$	Change in SOE
$\Delta\text{d}_{\text{trip}}$	Change in distance
DOC	Depth of cycle
DOD	Depth of discharge
EBSS	Energy content of battery
E_{year}^{pos}	Charged energy in the year
EFC	Equivalent full cycles
$\lvert I(t)\rvert$	Currently absolute current
n	Total number of time steps
$P(t)$	Current power
SOE	State of energy
SOC	State of charge
$\text{SOC}_{\text{cycle, start}}(t)$	State of charge at the beginning of a cycle
$\text{SOC}_{\text{cycle,end}}(t)$	State of charge at the end of a cycle
$u(t)$	Binary value of current temporal utilization
$\mu_{utilization}$	Temporal utilization ratio
μ_{V2G}	Temporal V2G-ready ratio
$v(t)$	Binary value of current V2G-ready ratio

the charging strategy by emulating the load profiles using three different charging strategies. Finally, part of this publication is an open-data repository including all BSS load profiles for each of the three modes of transportation.

In the following, we first describe the state of the art and existing literature before defining the research questions and presenting the scope of the work. In this work, the term e-Cars is used for cars instead of the often-used "electric vehicles" to distinguish between the electric vehicles of e-Cars, e-Buses, and e-Boats.

1.1. Summary of existing literature

In recent years, the electrification of cars, buses, and boats has been advancing [2–4]. Accordingly, research interest in these topics is also increasing. In the following, we summarize the literature on e-Cars, e-Buses, and e-Boats relevant to this paper. We then address vehicle charging strategies and the state of the art on relevant storage and battery KPIs.

E-Cars are a relevant topic, as they change not only the mobility sector but also the energy sector [2]. For this reason, research interest focuses on various issues of e-Cars, such as charging strategies, including fast charging and vehicle-to-grid (V2G), the influence on the distribution grid [7] and battery thermal management systems [8]. However, research also addresses the use of e-Cars and typical car loads. For example, an analysis of the user behavior and energy consumption of e-Cars was conducted by De Cauwer et al., in 2015 [9]. In their work, the authors analyzed GPS data from the EVA and Move platforms in Belgium and measured the energy consumption of a Nissan Leaf. For the e-Cars of their dataset, a range of 5000 to 6000 km per year was derived, which is less than the annual distances covered by internal combustion vehicles. They also showed that real energy consumption on the road might account for between 18 and 23 kWh/100 km – a value 30%–60% higher than the consumption measured by the New European Driving Cycle (NEDC). Similar trends were obtained by Hao et al., in 2020, who analyzed data from 197 e-Cars and determined energy consumption levels that were 7%–10% higher than those determined using NEDC [10]. A study by Chen et al., in 2020 evaluated data sets of 8000 e-Cars and plug-in hybrid electric vehicles (PHEVs) in Shanghai over a week and concluded that the e-Cars travel less than the PHEVs, averaging 32.6 km per day (compared to 36.3 km per day for the PHEVs) which is nearly 12,000 km per year [11]. Moreover, Tansini et al. conducted their tests on three e-Cars and determined consumption between 15 and 29 kWh/100 km with an average consumption of about 20 kWh/100 km [12]. In 2016, Zou et al. analyzed the driving behavior of taxi fleets consisting of 34 electrically powered taxis in Beijing [13]. On average, the taxis drove almost 118 km daily and consumed 11 to 30 kWh/100 km. The authors also analyzed battery charging characteristics and determined that 59% of the charging processes began between 30 and 50% SOC, and 74% were charged to an SOC higher than 90%. Consequently, the cabs were discharged by 40–70% during the trips. In the same year, Weldon et al. published a study of e-Car use in Ireland in which they evaluated eight privately used and seven commercially used e-Cars [14]. In contrast to Zou et al., the Weldon et al. study showed a wider distribution of SOCs at the start of charging: 58.7% of charging events started at an SOC between 50 and 100% [14]. However, this study used 2010 Mitsubishi i-MiEVs, which have a range of only 130 km. In addition, Zou et al. analyzed cabs, while Weldon et al. studied private and other commercially used e-Cars. Zhang et al. determined in a study of 55 e-Cars in Beijing that energy consumption depends on the outdoor temperature and that consumption is lowest at 15–20 °C [15]. They also showed that in Beijing, energy consumption was up to 10.26% higher for identical trips in winter than in the other three seasons. The descriptions of the state of research regarding e-Cars relevant to this work show that in practice they consume between 11 and 30 kWh/100 km and often cover smaller annual distances than internal combustion vehicles. Our work also presents the consumption and distances of a dataset of e-Cars but goes beyond this by evaluating and presenting further battery-relevant parameters.

In the literature, there are also studies of mobility behavior based on surveys. One is the "Mobility in Germany" study [16,17]. Results of the 2017 study were, for example, that on average, 3.1 trips and 39 km per person and day were made [17]. In addition, an e-Car in Germany is

used for 45 min per day on average, which means that it is not used almost 97% of the time [16]. Furthermore, the authors published statistics and probability distributions on mobility behavior in addition to these overall results. This data is used by *emobpy*, an open-source Python tool that can simulate the mobility behavior of e-Cars [18]. Since this tool is used in our work, we describe the simulation procedure and its parameters in chapter 2.

E-Buses have also gained importance in recent years, so annual publications on this topic have increased more than tenfold from 2008 to 2020 [19]. According to a review by Manzolli et al., the main trends of this research are vehicle and battery technology, fleet and energy management, and sustainability [19]. In the following, we focus on the research relevant to this paper on the driving behavior of e-Buses and the impact on battery systems. In 2015, Rogge et al. evaluated 1588 trips made by diesel buses operated by Stadtwerke Münster in Germany [20]. They used a method developed by Sinhuber et al. to dimension potential battery systems for the electrification of the buses and to simulate energy consumption [21]. The simulated energy consumption, including auxiliaries, ranged from 2.26 to 2.69 kWh/km, with a mean value of 2.47 kWh/km [20]. Three years later, in 2018, Gallet et al. evaluated 4135 e-Buses in Singapore, which traveled on average 186 km per day [22]. The mean value of the energy consumption was 1.75 kWh/km, with articulated e-Buses consuming an average of 2.47 kWh/km, double-decker consuming 2.34 kWh/km, and single-decker e-Buses consuming 1.62 kWh/km. At 1.35 kWh/km, Gao et al. also obtained similar consumption values [23]. In 2017, they published a framework evaluating diesel buses from Knoxville (USA) and using their driving patterns to simulate e-Buses. An evaluation of 99 e-Buses from seven cities in China was published by Wang et al., in 2020 [24]. They determined optimal speeds of 11–18 km/h to maximize battery efficiency using a random forest algorithm.

Furthermore, there is research on e-Buses that deals with charging management and associated degradation of the batteries. In 2018, Du et al. published an optimized control strategy for hybrid e-Buses to minimize life cycle costs by reducing battery aging [25]. Zhang et al. developed an optimized service and charging strategy for a fleet of e-Buses considering battery degradation and nonlinear charging profiles, which helped extend battery life by 47.2–96.1% [26]. They also found that the initial SOC when leaving the depot should be as low as possible for reduced degradation. In 2022, Manzolli et al. developed an optimization model for charging a fleet of e-Buses, including vehicle-to-grid (V2G) and consideration of battery degradation [27]. If battery replacement costs fall below 100 €/kWh, providing V2G with the e-Buses in the example country Portugal could become economically attractive. Analogous to the presentations of e-Cars, our work also extends the state of research on e-Buses concerning various battery-relevant parameters.

E-Boats are less of a focus of research than e-Cars and e-Buses, according to our research. Research focuses on designing and modeling pure and hybrid e-Boats [28–30]. In 2012, Spagnolo et al. published a design for an electric catamaran powered by photovoltaic (PV) and batteries [28]. Kabir et al. published a similar system for small ferries in Bangladesh in 2016 [29]. A year before, Soleymani et al. published a design and energy management of a 14-m hybrid e-Boat [30].

Another topic relevant to this work is vehicle **charging strategies**. The most straightforward charging strategy is the direct recharging of the vehicle after arrival at the charging station. We call this type of charging uncontrolled charging, analogous to our previous work and literature [31,32]. This type of charging places the vehicles in high SOC ranges, which has been shown to lead to higher calendar degradation of the batteries [33,34]. Smart charging of vehicles, in contrast, can reduce not only vehicle battery aging but also lower charging costs and reduce the concurrency of charging [35,36]. In 2016, Lacey et al. defined a delayed charging strategy where the vehicle was kept at low SOC after arrival and charged just before departure to reduce calendar degradation by lowering the average SOC [32]. In addition, the authors identified "less frequent charging" as another option to reduce calendar degradation by not charging after every trip. In 2017, Al-Karakchi et al. published a charging strategy with periodic pauses to reduce pressure and temperature [37]. This strategy reduced the capacity loss of exemplary LG 18650 cells by 2.5% after 350 cycles. Instead, Chen et al. let users choose between three charging strategies, in which users could obey or not obey grid scheduling depending on their risk preference [38]. Houbbadi et al. published a charging strategy for an e-Bus fleet in 2019, in which they optimized the charging behavior considering battery degradation [39]. The optimized strategy performed even better in capacity loss than a delayed strategy, which they called *postponed*, and far better than an uncontrolled charging strategy, which they called *greedy*. In addition to the unidirectional charging strategies presented, there are also bidirectional charging strategies in which vehicles participate in electricity markets using V2G [40,41].

Analysis of battery health and performance is crucial to developing cost-effective electric vehicles. Several **battery parameters** are well-suited for deriving stress factors and health indicators. As described, for example, the SOC influences the aging of the batteries [32,34]. Furthermore, depths-of-discharge (DODs) and temperature are relevant for battery aging [42,43]. Especially for cyclic aging, the charge rate (C-rate) is another relevant parameter, which is the current divided by the nominal capacitance [44]. The energy throughput or, in relation to the battery capacity, the number of equivalent full cycles (EFCs) also contributes to this type of aging [44]. The parameters mentioned are generally relevant for batteries in mobile and stationary applications [45]. As proposed in previous work, the utilization ratio of mobile storage systems allows quantifying the proportion of time a vehicle battery is used, either to provide mobility or for V2G provision [31].

Research has already addressed driving patterns and energy consumption of e-Cars and e-Buses. There is generally less research on e-Boats, and much of it relates to sizing and design. The research gap we have identified relates to the stress on the battery due to driving patterns in various modes of e-transportation. To the best of our knowledge, the impact of driving and charging behavior on parameters relevant to battery life and performance indication has been looked at with insufficient accuracy for e-Cars and e-Buses and not at all for e-Boats. This work aims to expand the publicly available knowledge about e-transportation. In addition, we found that no simulation tool exists that can be used to simulate different modes of e-transportation and quantify the stress on the battery system. Furthermore, vehicle usage profiles are scarce and rarely available as open data. We want to contribute to covering these research gaps in this paper and answer the following research questions (RQs):

RQ 1) How can various transportation modes be reproducibly simulated to obtain battery usage and health indications (Section 3.2)?
RQ2) How much energy do e-Cars and e-Buses consume in the exemplary datasets, and what is the influence of the ambient temperature on consumption (Section 4.1)?
RQ 3) What is the typical stress of mobile battery storage systems in various transportation modes regarding different parameters (Section 4.2)?
RQ 4) To what extent are battery-relevant parameters in mobile applications similar to stationary applications and could therefore similar cells be used in those applications (Section 4.3)?
RQ 5) What's the influence of charging strategies on the considered parameters (Section 4.4)?

1.2. Contribution and scope of this work

This work aims to analyze and compare various transportation means, which we also refer to as mobile storage applications, in the following. For this purpose, field data from e-Buses and e-Boats were collected, and data from e-Cars were simulated. The data is used to

emulate the three use cases in the simulation tool *SimSES* [6]. For this purpose, energy management systems (EMSs) were developed to track mobile storage systems' power or SOC profiles and simulate charging strategies at parking times. This extension of the prior published *SimSES* tool enables the simulation of mobile storage applications by others so that the storage behavior can be simulated and evaluated. Furthermore, we derive and analyze various storage parameters that allow comparison between the three transportation means. We also show the impact of different charging strategies on the parameters. To enable the use of the data of the three battery applications, e-Cars, e-Buses, and e-Boats, we provide the profiles as open data as part of this publication. With the help of these profiles, researchers and industrial partners can make their own simulations or evaluations of transportation means. Accordingly, the work provides the basis for further research in the field of e-transportation. Based on the work, battery technologies for the different means of transport can be compared and optimized for the respective application in the long term.

Fig. 1 shows an overview of the work. After a presentation of the data basis in chapter 2, the data processing and the simulation in SimSES is done in chapter 3. Chapter 4 presents the results of the work before chapter 5 gives a summary and an outlook.

2. Database

For the present work, data on various mobile storage applications were collected and processed. The specifications of the raw data sets are shown in Table 1. To achieve a large number of data sets from privately used EVs, the simulation tool *emobpy* from DIW Berlin is used [18]. This tool uses statistics on the driving behavior of private individuals in Germany and the standardized driving cycles WLTC (Worldwide harmonized Light-duty vehicles Test Cycles) and EPA (Environmental Protection Agency) to simulate the use of e-Cars. For example, it can simulate effects on the electricity grid due to charging behavior. For the present work, *emobpy* was extended together with DIW Berlin so that the power demand during trips can now be tracked to the second. To determine different driving profiles and power requirements of the e-Cars, various trips were simulated in *emobpy*: First, the three driver types of commuters, non-commuters, and free-time drivers were selected. The driving behavior of each of these three driver types was simulated over one year in ten simulation runs to account for a wide range of driving profiles determined by probability distributions. A time resolution of 60 s was chosen to reduce the duration and memory requirements of the simulations. Germany's mean hourly resolved temperature was used as the ambient temperature in the simulations. In general, emobpy allows the selection of one of 39 European countries as simulated ambient temperature [18].

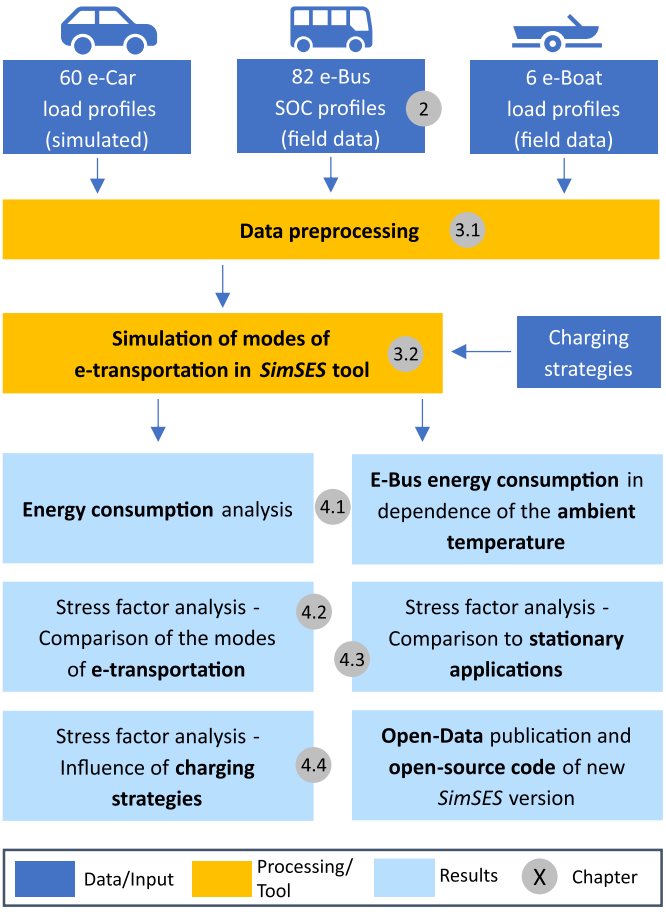

Fig. 1. Structure of the work and respective chapter number.

Table 1
Datasets of the different transportation means.

	e-Car	e-Bus	e-Boat
Number of datasets	60	82	6
Origin	Simulated	Measured	Measured
Available data	Power, distance	SOC, milage, ambient temperature	SOC, power
Length of datasets	One year	One day to 14 months	3–9 months
Time	2021	2021–2022	2021
Sampling rate	60 s	10 s	5 s
Data resolution	Power: values derived from trips' energy consumption distance: 1 km for trips	SOC: 0.01% to 0.5% mileage: 0.1 km temperature: 0.1 °C	SOC: 1% power: 10 W
Industry/ Research Partner	*emobpy* (DIW Berlin) [18]	Hochbahn Hamburg	Torqeedo

Then, in the second step, the power profiles for the e-Cars were simulated for the two vehicle models, Volkswagen ID.3 (2020) and Tesla Model 3 (2020), using the three simulated driver types. These models were selected because they were among Europe's top three best-selling e-Car models in 2021 [46]. The results are a total of 60 e-Car load profiles. In addition to the load profiles, binary profiles were extracted that indicate whether the vehicle is parked at home or on the road. These binary profiles are used in *SimSES* to map the charging behavior with different charging strategies. Table A1 in the appendix shows the characteristics of the vehicles used for the simulation of the three applications. The assumed charging power for the e-Cars is 11 kW. We describe the use of these parameters for the *SimSES* simulation in section 3.2.

For the mobile application of e-Buses, data was exchanged with Hochbahn Hamburg, which is converting its entire bus fleet to e-Buses by 2030 [5]. Hochbahn Hamburg provided the SOC profiles of 82 e-Buses over up to 14 months for this work. The mileage, speed, and outside temperature were also measured and transmitted with the SOC data. The SOC profiles have a sampling rate of 10 s once the e-Bus is switched on. If the e-Bus is switched off, the SOC is not recorded. Thus, the charging behavior is not tracked. The six e-Bus models available in the dataset are listed in Table A1. For example, there are nine e-Buses from the manufacturer Evobus with Nickel–Manganese–Cobalt (NMC) lithium-ion batteries and a useable capacity of 190 kWh each. The total number of e-Buses in the table is 52, as 30 e-Buses are filtered out by the data processing described in section 3.1. We apply 150 kW as the maximum charging power at the bus depot for e-Buses with NMC battery and 80 kW for e-Buses with Lithium-metal-polymer (LMP) battery, as these are the charging power values of Hochbahn Hamburg. As the maximum power that can be charged and discharged from the batteries,

we apply 350 kW.

The third mobile application of batteries considered in this work is e-Boats. To analyze this application, we collaborated with Torqeedo, who develops and sells electric propulsion systems for e-Boats. Torqeedo provided data from six e-Boats over three to nine months (see Table A1). These six e-Boats represent a smaller database compared to the e-Cars and e-Buses. However, the datasets include ferries and private boats, so a range of exemplary electric boats can be represented. The data includes the SOC and the power balance with a resolution of 5 s. In contrast to the e-Cars and e-Buses, no information is available about the distances traveled. Table A1 also shows the battery capacity and power of the e-Boats. The capacities of the small e-Boats (1–2 t) are 30–40 kWh. In contrast, the large e-Boats (7.5–37 t) have capacities between 80 and 160 kWh. Regarding technical implementation, the 160-kWh e-Boats consist of four 40-kWh battery packs and the 80-kWh e-Boat consists of two 40-kWh battery packs. In the field, this allows variably connecting or disconnecting packs. We neglect this flexibility in this work and assume 160 kWh and 80 kWh battery packs for our simulations. The maximum powers are between 100 and 250 kW. Since the charging power of the e-Boats depends on the respective user and varies over time, we take the most frequently occurring charging power resulting from the load profiles as the standard charging powers. However, the most frequently occurring charging powers for Boat B and Boat C are 40 W and 630 W, respectively. For these two e-Boats, we specify 7 kW as the minimum power, so the most frequently occurring charging powers are 7.82 kW and 32.53 kW, respectively. These charging powers appear realistic for e-Boats with capacities of 80–120 kWh.

3. Methodology

This chapter focuses on the methodology of the work. First, section 3.1 deals with the preprocessing of the raw data. Then, section 3.2 explains the simulation of mobile storage applications in SimSES, including the charging strategies. Finally, section 3.3 describes relevant storage parameters used in the results to compare the mobile applications with each other and with stationary applications.

3.1. Preprocessing and analysis of raw data

As described in chapter 2, *emobpy* is extended to simulate the **e-Cars** so that the load during trips is also recorded and saved. The output of *emobpy* is 60 annual power profiles and binary profiles for the two vehicles and three driver types (compare Table 1 and Table A1). For the preprocessing, the software MATLAB was used. A first analysis of the raw data is provided in Fig. 2, which shows two histograms of the average daily distances traveled by the e-Cars. In light orange, the annual distance driven by each e-Car is normalized to the total number of 365 days. In orange, the yearly distance is normalized to the number of days with driving activity. Overall, the simulated e-Cars travel 21–31 km per day on average. On a day with vehicle usage, the average distance is between 36 and 50 km. The distances traveled by the e-Cars in a year consequently range between 7700 and 11,100 km. Compared to the average mileage in Germany, which is 13,000 km, the private e-Cars simulated have relatively small mileages [47]. According to the developers of *emobpy*, one reason could be that the study *Mobility in Germany*, whose data the tool uses, only asks for distance categories of individual trips, e.g., “trip over 150 km”. Moreover, studies have shown that e-Cars often drive shorter distances than internal combustion vehicles. For example, De Cauwer et al. determined around 5500 km as the annual distance of two pure electric vehicle fleets in 2015 [9]. In their study from Ireland, Weldon et al. obtained 26–33 km per day (9490 to 12,045 km per year) [14]. Chen et al. found 32.63 km per day (11,900 km per year) for e-Cars in Shanghai [11]. Based on these study results, we accept the deviation from the mean value of the annual distance driven by e-Cars in Germany at this point.

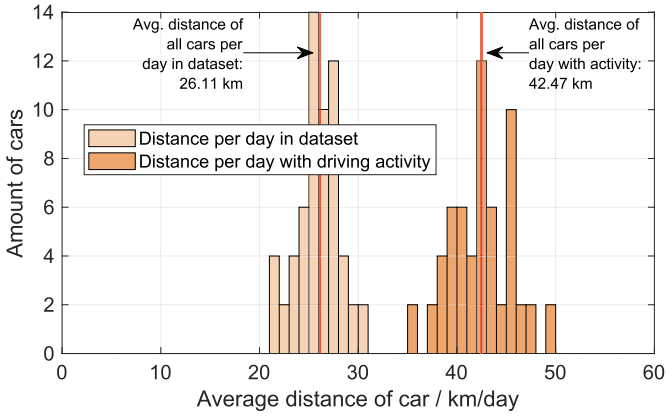

Fig. 2. E-Car dataset (60 e-Cars): Histograms of e-Car average trip distance in km per day normalized to total number of days (light orange) and normalized to only days with driving activity (orange), respectively. (For interpretation of the references to colour in this figure legend, the reader is referred to the Web version of this article.)

The original **e-Bus** data is partitioned by day and is divided into individual CSV files for each e-Bus as a first step. Those files contain a timestamp and the SOC. In addition, a CSV is formed from timestamp and outdoor temperature, which allows an analysis of the influence of temperature on energy consumption in the further course of the present work (see section 4.1). Moreover, the following metadata is saved for each e-Bus: Bus number, bus manufacturer, battery type (NMC or LMP), useable battery capacity, average distance driven per day in kilometers, start time, and end time. Next, a data cleansing was performed in which requirements were defined that the individual e-Bus data records must fulfill to filter out small records and records with significant gaps (see

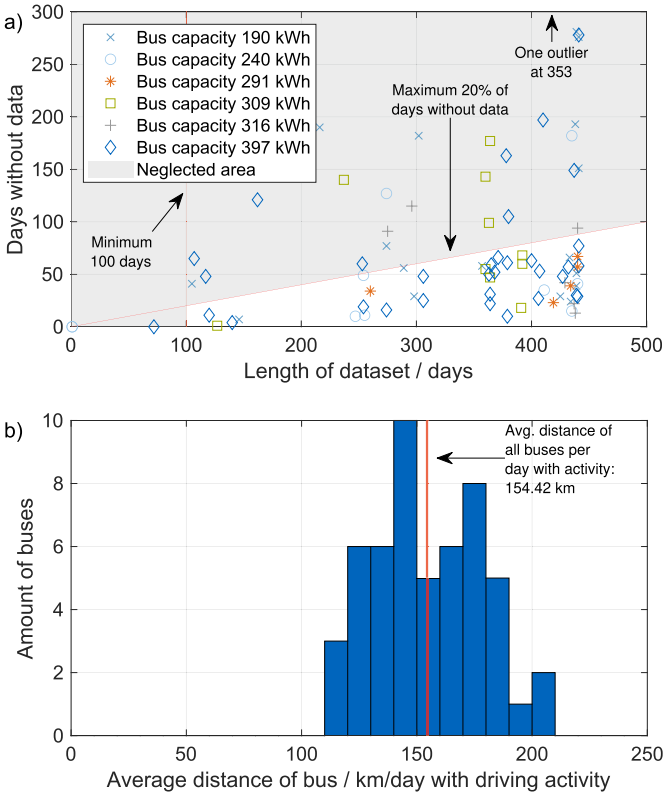

Fig. 3. E-Bus data analyzed - cleansing (a) and cleaned data analysis (b). (a) Scatter plot showing the days without data between the first and last day of a dataset over the total length of the dataset. (b) Histograms of the average driven distance in km per day for days with driving activity.

Fig. 3 a). Each e-Bus record must therefore contain at least 100 days of data. In addition, at most 20% of those days may be without recorded activity. On the one hand, days without activity may be due to the normal break days since fewer city e-Buses are used on weekends compared to workdays. On the other hand, the e-Buses may also be in the repair shop on these days. In addition, errors could also have occurred during data acquisition. For this reason, all e-Buses with more than 20% of inactivity are filtered out. This data cleansing leaves 52 e-Buses that meet the requirements. Fig. 3 b shows a histogram of the distances driven per day with driving activity, analogous to Fig. 2. The 52 filtered e-Buses travel between 113 and 207 km per day with recorded trips. If the e-Buses were used daily, this would correspond to an average of 56,210 km per year. Including the non-operating days, the e-Buses travel 94–189 km per day. This would correspond to 50,735 km per year.

To simulate mobile applications, *SimSES* requires a binary profile in addition to a power or SOC profile. This binary profile indicates whether the vehicle is connected to the grid at a certain point in time (1) or not (0). When the vehicle is connected, it can then be charged according to charging strategies, further explained in the following section. The raw data already includes information on whether the e-Car is currently not at home but on the road, at work, shopping, or at home. In this work, only at-home times are interpreted as possible charging times. Since the binary profile does not exist for the e-Buses and e-Boats, it is generated for each SOC respectively load profile separately, as explained in appendix section 6.2.

The six **e-Boat** datasets include three to nine months of data. The e-Boat types with battery capacity and power are shown in Table A1. Analogous to the e-Cars and e-Buses, the raw data of the e-Boats is evaluated in the following. Fig. 4 shows the distribution of recorded driving activity for all six e-Boat types. The white spots in between describe periods (days, weeks, or months) without recorded data. After consultation with Torqeedo, the gaps are not errors but show regular periods without activity. In contrast to the e-Car and e-Bus data, the e-Boat data does not include traveled distance measurements. The storage simulation tool *SimSES*, described in the following section, allows the simulation of the storage behavior in different temporal resolutions. If gaps occur in the data, *SimSES* interpolates between the last and the next data point. In the e-Boat simulations, this results in e-Boats being continuously discharged over several days and weeks when no data was available. To prevent this, power values of 0 W were inserted at the beginning and end of gaps with more than 1-h durations. This causes the simulated boot to stay idle in accordance with the original data.

3.2. Simulation of mobile applications in SimSES

The storage simulation tool *SimSES* has been developed at the Chair of Electrical Energy Storage Technology at the Technical University of Munich [6]. It enables the simulation of stationary energy storage systems in various applications. The time series simulation is complemented by a techno-economic analysis in which, e.g., efficiency and battery degradation are evaluated. *SimSES* can be used, for example, to simulate stationary home BSSs in self-consumption-increase (SCI) application and large-scale stationary BSSs in the frequency containment reserve (FCR) application. For the present work, *SimSES* is extended toward mobile BSSs. Mobile BSSs are, for example, e-Cars, e-Buses, and e-Boats that are temporarily used for mobility and are temporarily connected to the power grid. For this reason, *SimSES* first requires the binary profile to simulate the vehicles. Next, it requires the load or SOC profile during times when the vehicle is not connected to the grid. This is especially relevant since vehicles are not always connected when they are parked. For the simulation of mobile applications, *SimSES* follows the load profile during the on-the-road times. The resolution used in the simulations is the resolution of the original data shown in Table 1. If the vehicle is connected, charging occurs according to a specified charging strategy. This fundamental principle applies to all mobile applications considered in this work. However, since data on the e-Buses is only available as SOC values, an energy management system (EMS) based on SOC data (SOC-EMS) is developed in addition to a power-based EMS (Power-EMS). In this strategy, the storage system follows the SOC data when the binary value is zero and allows charging according to similar charging strategies as in the power-based EMS when the binary value is one. For this purpose, the EMS calculates the required battery power from the SOC value to reach the desired SOC in each timestep. This approach approximates the real battery power but depends on the resolution of the SOC and the sampling rate. Real power peaks are thus not captured on the one hand, and unrealistic power peaks can occur on the other hand due to short peaks in the SOC profile. The resolution of the e-Bus SOC models is given in Table A1 in the “other info” column. A difference between the Power-EMS and SOC-EMS is that the charging strategies in SOC-EMS charge to a target SOC at the time of departure. This is necessary because otherwise, more significant discrepancies between the SOC in *SimSES* and the original SOC could occur during the next trip, which *SimSES* compensates for with high-power charging or discharging. In the case of the Power-EMS, the battery is charged to 100% SOC until departure since the target SOC is unknown.

Three charging strategies have been implemented in the adapted version of *SimSES*, as depicted in Fig. 5: An uncontrolled charging strategy (a), a mean-power charging strategy (b), and a paused charging strategy (c). In uncontrolled charging, the vehicle is charged at maximum power up to 100% SOC (Power-EMS) or to the target SOC (SOC-EMS) immediately after connection to the electricity grid. In mean-power charging, perfect foresight determines when the vehicle will leave and charge accordingly with the power required to reach 100% SOC or the target SOC at departure time. In paused charging, the vehicle is charged to a minimum SOC immediately upon arrival (e.g., 60%), and subsequently, the charging process is paused. If the SOC at arrival is already above the specified minimum SOC, the current SOC is kept constant, as displayed in the night of January 26th in Fig. 5. During the pause, the EMS determines in perfect foresight when the vehicle will depart. Accordingly, the charging process continues at maximum power so that the vehicle reaches 100% SOC or the target SOC (SOC-EMS) at the time of departure. If 100% is set as the minimum SOC during the pause, this corresponds to the uncontrolled charging strategy. The other extreme is 0% minimum SOC during the pause. In this case, the vehicle would always hold the current SOC after arrival and only charge to 100% SOC or the target SOC shortly before departure. This work’s selection of charging strategies represents a sample of possible non-optimized charging strategies. In the field, aggregators of vehicles would develop optimized charging strategies. Examples of charging strategies with optimization algorithms would be minimizing electricity costs, minimizing distribution grid load, or minimizing battery degradation [32,33,35].

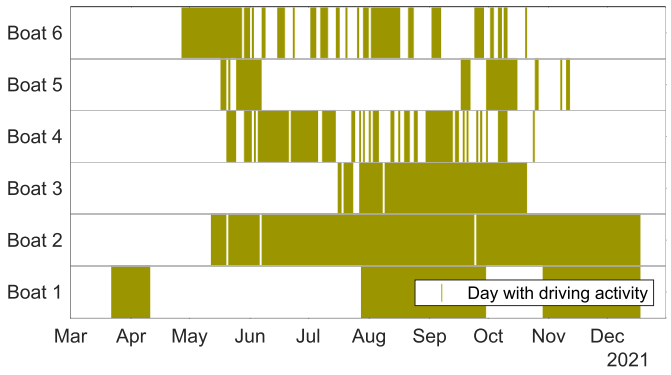

Fig. 4. E-Boats database - days with driving activity are green, and days without driving activity or no data are white. (For interpretation of the references to colour in this figure legend, the reader is referred to the Web version of this article.)

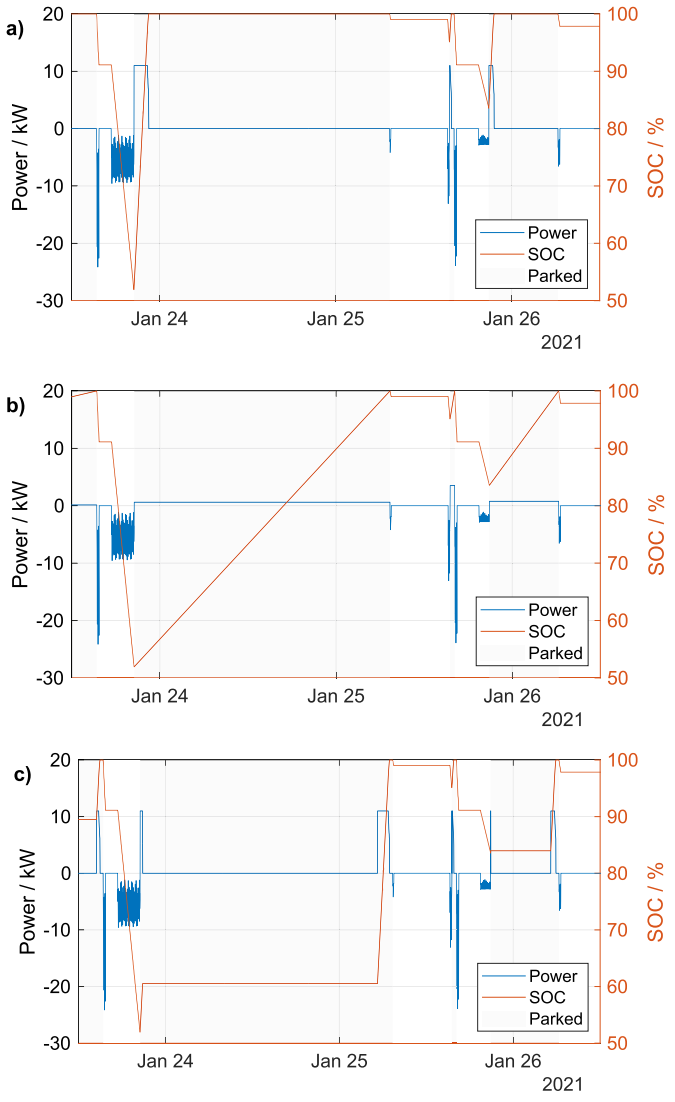

Fig. 5. Illustration of the three charging strategies for an exemplary time snapshot. a) Uncontrolled charging, b) mean-power charging, c) paused charging.

The Power-EMS has a unique feature: If the SOC drops below 2% during a long drive, a fast charge with 150 kW to 80% SOC is simulated. For this purpose, a fast-charging station is assumed to be available on these trips. The trip is postponed by the charging time and is continued after the charge. With the SOC-EMS, implementing fast charging is not required since the SOC profile would already have included the fast-charging process during a long trip. For the Power-EMS, the simulation of fast charging is necessary because, with small vehicle batteries, the desired driving distance might not be achieved with only home charging.

For the simulation of the mobile applications, the battery model of a lithium-ion NMC cell was used [42]. In addition, an inverter model by Notton et al. was applied [48]. The technical specifications of the battery cell are shown in Table A2 in the appendix.

3.3. Relevant mobile storage parameters

Storage systems can be characterized and evaluated in different applications with various parameters (see Section 1.1). In the following, we define the parameters used in this work.

The SOC of a storage system is defined as the fraction of the currently charged electrical charge ($C_{act}(t)$) to the total possible capacity ($C_{total}(t)$) as displayed in equation (3.1). $C_{total}(t)$ is also time dependent since the total capacity of the battery reduces over time due to degradation effects. Over the entire duration of the simulation or the profile, there is a value for the SOC at every point in time. In our evaluations in section 4, we determine each vehicle's mean SOC for the different transportation modes. We also determine the SOC at the end of each trip, before the vehicle is connected to the electricity grid, i.e., the binary value becomes one. The SOC is relevant for lithium-ion batteries because both calendar and cyclic degradation depend on it [42–44]. High SOCs tend to lead to accelerated calendar aging [42,43], while cycling in high and low SOC ranges may lead to accelerated cyclic aging compared to a mid-range of 45–55% SOC [42]. In general, battery degradation depends on the individual cell type, but the SOC is often a relevant stress factor in battery degradation modeling [49]. For the e-Buses, the useable capacity is used as $C_{total}(t)$, as the tracked SOC data ranges from 0 to 100%. However, the tracked SOC could deviate from the real battery SOC if the bus manufacturer only releases a certain voltage range to be used.

The following parameter is the depth of cycles (DOCs), determined according to equation (3.2). For this purpose, it is calculated for each cycle how deep the battery was charged or discharged. The cycles can be determined in different ways. In *SimSES*, a half-cycle detector is implemented [6]. Another possibility would be, for example, the use of a rain flow counting algorithm [50]. Here, a distinction can also be made between the charging and discharging direction. The term depth of discharge (DOD) is often used in the discharging direction. Analogous to the mean SOC at the end of trips, we determine the mean DOD of the trips by subtracting the SOC at the beginning of each trip from the SOC at the end of the trip.

Another relevant parameter is the C-rate, which describes the current (I) at which the battery is charged or discharged in relation to its total capacity (C_{total}). The calculation of the C-rate is shown in equation (3.3). It can be calculated as an absolute value as in the equation or separately in charge and discharge direction. As described in section 2, the e-Bus data consists of SOC values. In *SimSES*, these SOC values are tracked during the trips, and the power is determined in each time step that must be charged or discharged to reach the target SOC. The current can then be used to determine the C-rate. We use the original power profiles for the e-Car and e-Boat data to determine the current directly from the power, not from a SOC profile. The cycles that the battery completes over a period of time are often referred to as equivalent full cycles (EFCs) or full equivalent cycles (FECs). Equation (3.4) describes the EFC calculation as implemented in *SimSES* [45]. For this purpose, the charged energy in the year (E^{pos}_{year}) is divided by the energy content of the battery (E_{BSS}).

Especially for mobile applications, another parameter is of relevance: The temporal utilization ratio $\mu_{utilization}$, the calculation of which is given in equation (3.5) and described in detail in [31]. This parameter represents the proportion of time a battery is charged or discharged in an application. For this purpose, the sum of the time steps at which the power $p(t)$ is not equal to zero is divided by the total number of time steps n. For vehicles, this ratio means the proportion of time the vehicle is discharged due to trips or charged. The rest of the time, the vehicle is not used and is either parked somewhere on the road or at the charging point without being charged. In Germany, for example, a study found that private cars are parked for more than 23 h per day on average, resulting in a utilization ratio of less than 5% [16]. For stationary BSSs, the temporal utilization ratio describes the proportion of time that the BSS is charged or discharged. The rest of the time, the BSS is connected but not in use.

The final parameter relevant to the transportation means is the temporal V2G-ready ratio μ_{V2G}. This parameter indicates the proportion of the time the vehicle is connected to the electricity grid but not being charged. The calculation of μ_{V2G} is shown in equation (3.6). Accordingly, the auxiliary variable v (t) is one if the vehicle is neither charged nor discharged ($P(t) = 0$) and the binary value is one ($b(t) = 1$). For the e-

Bus, b(t) = 1 means that the e-Bus is in the depot, for the e-Car that it is at home, and for the e-Boat that it is at the dock. The variable μ_{V2G} is not simply one minus $\mu_{utilization}$, since the vehicles can also be on the road without being charged or discharged or without being connected to the electricity grid. With the help of μ_{V2G}, it is possible to estimate the temporal V2G potential of the vehicle. At this point, V2G is representative of all forms of power feedback from the vehicle, including vehicle-to-home (V2H), for example.

$$SOC(t) = \frac{C_{act}(t)}{C_{total}(t)} \tag{3.1}$$

$$DOC = SOC_{cycle,start} - SOC_{cycle,end} \tag{3.2}$$

$$C_{rate,abs}(t) = \frac{|I(t)|}{C_{total}(t)} \tag{3.3}$$

$$EFC = \frac{E^{pos}_{year}}{E_{BSS}} \tag{3.4}$$

$$\mu_{utilization} = \frac{\sum_{t=1}^{n} u(t)}{n} \tag{3.5}$$

$$\mu_{V2G} = \frac{\sum_{t=1}^{n} v(t)}{n} \tag{3.6}$$

$$\text{With: } u(t) = \begin{cases} 1, P(t) > 0 \vee P(t) < 0 \\ 0, P(t) = 0 \end{cases}.$$

$$v(t) = \begin{cases} 1, P(t) = 0 \wedge b(t) = 1 \\ 0, otherwise \end{cases}$$

3.4. Procedure for determining e-bus energy consumption in dependence on the ambient temperature

The e-Bus data includes not only the SOC profiles but also data on the mileage and the ambient temperature of the e-Buses. In Section 4.1, the energy consumption of the e-Buses is determined as a function of ambient temperature. Therefore, a combination of raw data (mileage and ambient temperature) and simulation results (energy consumption) from *SimSES* is used. To obtain a complete dataset for the e-Bus mileage, forward filling is used since the mileage is not recorded at each time sample. The *SimSES* simulations are performed with a resolution of 10 s, which can be directly matched with the raw data samples. Thus, the entire dataset contains the ambient temperature, e-Bus mileage, battery SOCs, and states of energy (SOEs). Here, the SOE indicates the total amount of electrical energy in kWh contained in the battery. For further analysis, the data is split into individual *trips*. Trips are time intervals during which the e-Buses are not connected to the grid, and an increase in mileage is observed. To disregard times when the e-Buses are connected to the grid, we check the binary value for $b(t) = 0$. Additionally, we defined the following criteria for a valid trip:

- 2 h < trip duration <24 h
- 20 km < trip distance <300 km

Trips of less than 2 h and 20 km are neglected to ensure no service or test drives are considered. In regular operation, e-Buses are charged each night. Trips of more than 24 h are disregarded to disregard unusual operation. Finally, a bug in logging the mileage led to unreasonable jumps in the mileage counter. Overall, the analyzed e-Buses usually cover between 84 and 130 km in a complete shift of 8 h. Thus, an upper limit of 300 km is appropriate to filter out faulty mileage readings without neglecting valid trips. This procedure yields more than 22,000 trips for all 52 e-Buses.

During each trip, the e-Bus undergoes a change of SOE and mileage. The average energy consumption for each trip is computed as the fraction of change in SOE (ΔSOE) and distance driven (Δd):

$$Consumption_{trip} = \frac{\Delta SOE_{trip}}{\Delta d_{trip}} \tag{3.7}$$

Additionally, the mean ambient temperature of each trip is computed to allow for the analysis of ambient temperature-sensitive energy consumption behavior.

4. Results

This chapter presents the results of our work. Section 4.1 describes the results on the energy consumption of the individual mobile applications. In addition, we provide an in depth-analysis of the consumption of the e-Buses depending on the ambient temperature. Section 4.2 compares the effects of the applications on the batteries with each other using the parameters presented. Subsequently, we compare these with the parameters of stationary applications in section 4.3. Lastly, the influence of the charging strategies on the parameters is shown in section 4.4.

4.1. Energy consumption analysis of e-cars and e-buses

This section shows the energy consumption results of the three transportation modes. At this point, the energy consumption refers only to the DC side and neglects, for example, charging losses. Fig. 6 a) shows the total energy consumption of the e-Cars over the distance traveled. The simulations were performed with *emobpy* over one year, and the models chosen are the Tesla Model 3 and the Volkswagen ID.3 (see section 2). As described in section 3.1, the distances traveled range from 7700 to 11,100 km. The Tesla and the Volkswagen were simulated for each mobility behavior, resulting in each distance value occurring once in the diagram for each vehicle type. The energy consumed by the e-Cars was determined in *SimSES* and ranges from 1450 to 3200 kWh. The two lines in the graph indicate consumptions of 20 kWh/100 km and 30

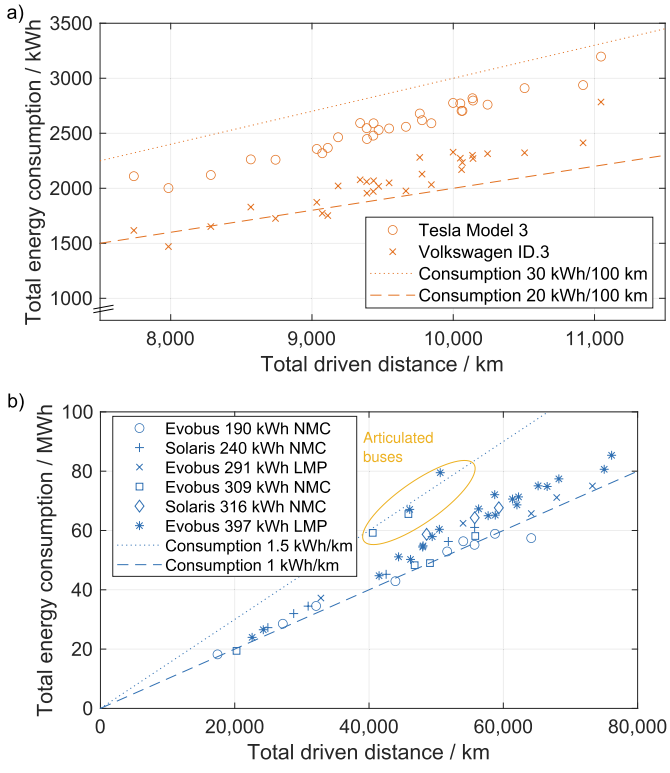

Fig. 6. a) Simulated e-Car energy consumption analysis separated by model. Tesla Model 3 avg. consumption: 26.78 kWh/100 km; Volkswagen ID.3 avg. consumption: 21.38 kWh/100 km. b) E-Buses energy consumption analysis separated by e-Bus types.

kWh/100 km. Per 100 km, the e-Cars' energy consumption is between 18 and 29 kWh. The Tesla Model 3 has a higher consumption than the Volkswagen ID.3, in line with previous results [18].

Fig. 6 b) shows the energy consumption of the e-Buses over the distances driven, broken down by the e-Bus types. In contrast to the e-Car data, the e-Buses were not all measured over the same period (see Fig. 3 a). This increases the differences in the distances traveled by the e-Buses. Consequently, the e-Buses have traveled between 17,400 and 76,200 km. Analogous to Fig. 6 a), the two lines show exemplary energy consumption rates of 1 and 1.5 kWh/km. The diagram indicates that most e-Buses show an average consumption of 1–1.2 kWh/km. Four e-Buses show increased consumption of 1.4–1.6 kWh/km. These e-Buses are articulated buses, which explains the increased consumption. Apart from that, we did not find significant differences in average consumption between the different e-Bus models. Compared to the literature, the studied e-Buses investigated in this work show relatively low energy consumption (see section 1.1). On the one hand, this may be because the studied e-Buses are from the construction years 2019–2021, while the cited papers were published between 2015 and 2018 and therefore show older bus models. On the other hand, our results show only DC-side consumption, while other articles include charging losses in some cases. Moreover, Rogge et al. used a simulation model, not field data from e-Buses, and came up with over 2.2 kWh/km energy consumption in 2015 [20]. In 2017, Gao et al. already determined consumptions of 1.35 kWh/km for real e-Buses [23]. Lastly, the outdoor temperature significantly impacts energy consumption, as shown in more detail below. This can result in different energy consumption rates for identical e-Buses in different countries.

Fig. 7 also illustrates the consumption of the e-Cars and e-Buses per kilometer as boxplots, classified according to the models. The Volkswagen ID.3 consumes, on average, between 0.184 and 0.25 kWh/km, while the Tesla Model 3 is between 0.25 and 0.29 kWh/km. The e-Buses consume, on average, between 0.89 and 1.58 kWh/km. E-Buses with smaller batteries tend to consume less energy than larger e-Buses, although the spread in the individual segments is relatively large in some cases. For example, the six 240-kWh e-Buses consume between 1.06 and 1.11 kWh/km, while the six 309-kWh e-Buses consume between 0.96 and 1.46 kWh/km. The two outliers in the 397-kWh e-Bus segment are two articulated e-Buses from Fig. 6 b). The two other outliers in Fig. 6 b) form the maximum in the 309-kWh e-Bus segment. Other reasons for differences in individual e-Bus consumption could be external influences, such as the outside temperature or route-characteristics, in addition to the general driving style. We, therefore, perform an analysis of consumption depending on the outdoor temperature in the following paragraphs.

As described in section 2, the e-Bus data contains values for the ambient temperatures of the e-Buses. Therefore, we analyze the trip energy consumptions of the 52 e-Buses described in Section 3.1 in dependence on the ambient temperature according to the methodology explained in Section 3.4. Each trip thus yields an average trip consumption and an average ambient temperature. All trips are weighted equally for the boxplots in Figs. 8 and 9.

Fig. 8 shows the energy consumption of all trips in dependence on the average trip ambient temperature from 10 to 30 °C. Generally, e-Buses show minimal consumption at 20–22 °C. The analysis of all e-Buses and their respective trips yields the lowest median consumption at 21 °C with a value of 0.98 kWh/km. Consumption increases for higher temperatures mainly due to air conditioning. The e-Buses show an increase to a median consumption of 1.16 kWh/km at an ambient temperature of 30 °C (+19%). For decreasing temperatures, electric heating shows an analogous increase in energy consumption. At 10 °C, a median consumption of 1.24 kWh/km (+27%) can be observed. Overall, the e-Bus energy consumption increase is almost symmetric regarding temperature variation from 10 to 30 °C. As a rule of thumb, energy consumption increases by 2–3% per 1 °C change in ambient temperature.

Fig. 9 shows the resulting consumption behaviors depending on the ambient temperature for the two specific types of e-Buses, Solaris 240 kWh and Evobus 309 kWh (excluding the two articulated buses of this type). The boxplots of the other four types are displayed in Appendix Fig. A2. The consumptions of the individual e-Bus categories reveal an almost identical behavior above 14 °C. At lower temperatures, the trends differ substantially. E-Buses of type Evobus 309 kWh show the expected behavior of increasingly higher consumption at lower ambient temperatures. The lowest median consumption of this type is found at 22 °C with 0.89 kWh/km. At −2 °C, the median consumption doubles to 1.77 kWh/km. E-Buses of type Solaris 240 kWh have a minimum consumption of 0.94 kWh/km at a temperature of 21 °C. The consumption climbs for decreasing temperatures to a maximum median value of 1.37 kWh/km at 8 °C, an increase of 46%. A sudden drop to a median consumption of 1 kWh/km is observable for temperatures below this threshold. The reason behind this divergence is the heating method. All E-Buses in this analysis contain a hybrid heating solution consisting of an electric heater and fossil fuel heating. The operation strategy of the latter differs between bus manufacturers. In this analysis, Solaris' 240 kWh e-Buses seem to switch to exclusive fossil fuel heating when the temperature drops below 8 °C. Such an operation strategy conserves battery to extend the driving range but has the disadvantage that these e-Buses remain dependent on fossil fuels.

4.2. Comparison of mobile applications

Following the analysis of e-Car and e-Bus consumption, this section compares the stress on the batteries in the three mobile storage applications. Fig. 10 (a) shows the distributions of the energy consumption of

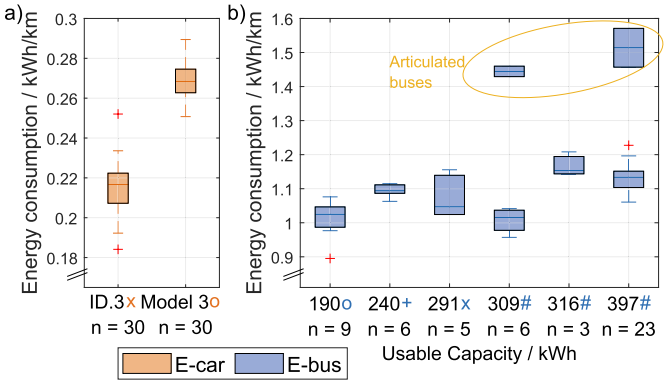

Fig. 7. Simulated e-Car (a) and field-data e-Bus (b) boxplots of the vehicle mean energy consumption per kilometer for the different models. The symbols next to the type correspond to the symbols in Fig. 6. The numbers below the types indicate the number of car or bus types in the data sets.

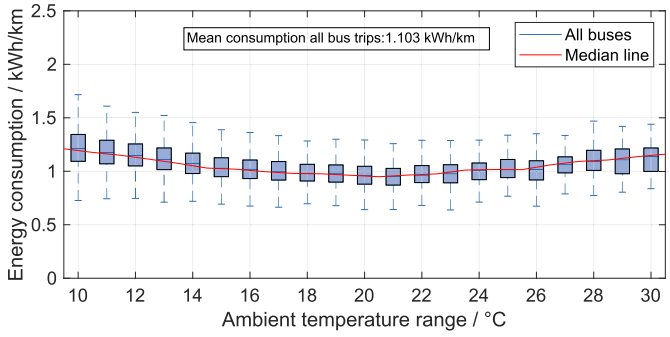

Fig. 8. Boxplot diagram of the energy consumption depending on the ambient temperature for all e-Busses of all categories. Outliers are removed to not distract from the general trend. The complete diagram with outliers is displayed in Appendix Fig. A1.

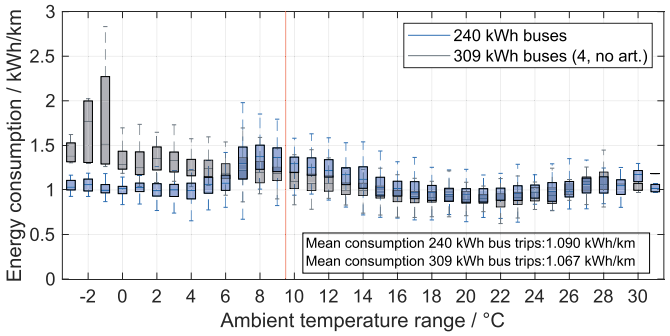

Fig. 9. Boxplots of the energy consumption of the e-buses "Solaris 240 kWh" and "Evobus 309 kWh" in dependence on the outside temperature. The red vertical line indicates the X-axis limit from Fig. 8. Outliers are removed to not distract from the general trend. The complete diagrams with outliers are shown in Appendix Fig. A2. (For interpretation of the references to colour in this figure legend, the reader is referred to the Web version of this article.)

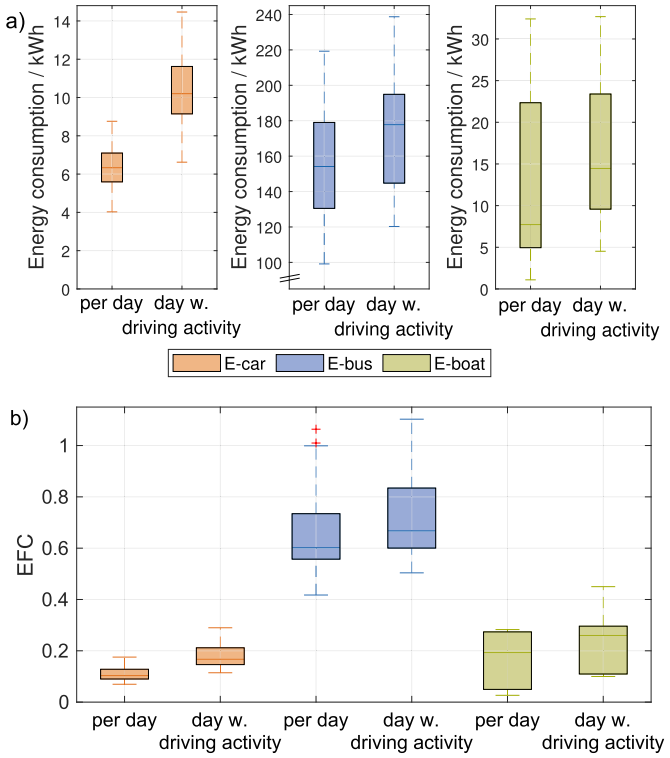

Fig. 10. Boxplots showing energy consumption (a) and equivalent full cycles (EFCs) (b) for all vehicle types analyzed. Data normalized per day and per day with driving activity.

the three means of transport as boxplots. The left boxplot indicates the average energy consumption of the vehicles per day over the respective dataset length. The boxplot on the right shows the average daily energy consumption on which driving activities occurred. The simulated e-Cars thus consume a median of 6.3 kWh per day. On days when the e-Cars are used, they consume a median of 10.1 kWh. In contrast, the e-Buses consume 99 to 220 kWh per day. Since the e-Buses drive more frequently than the e-Cars, the right boxplot of the e-Busses differs only slightly from the left boxplot. The energy consumption of the e-Boats shows the most significant spread. There are e-Boats that consume, on average, only 1 kWh per day and e-Boats that consume 32.5 kWh per day. One reason for this could be the significant differences in e-Boat sizes. For example, the lightest e-Boat weighs only 1 ton, and the heaviest is 37 tons (see Table A1). In addition, the e-Boats drive with different frequencies. The e-Boat that needs only 1 kWh per day consumes 4.5 kWh on days with trips and thus forms the minimum in the right boxplot. In contrast, the e-Boat that consumes 32.5 kWh per day also travels almost daily, so the maximum of the right boxplot is 32.8 kWh.

Below, Fig. 10 (b) shows the EFCs of the three means of transport also as boxplots and once per day and once per day with driving activity. As the battery capacities of the three means of transport vary, the daily EFCs do not differ as much as the energy consumption in Fig. 10 (a). The simulated e-Cars make between 0.07 and 0.18 EFCs per day with a median of 0.102 EFCs. The median value corresponds to about 37 EFCs per year. If only the days on which trips occurred are considered, the EFCs increase by 50%–70% for the e-Cars. The e-Buses make more EFCs despite having larger battery capacities ranging from 190 to 397 kWh. The median here is 0.60 EFCs per day and 0.67 EFCs per day with driving activity. Since the e-Buses run on more days than the e-Cars, the EFCs per day of driving activity only increase by up to 23%. At the peak, there are even e-Buses that make a mean of 1.1 EFCs on the days they operate. Accordingly, if an e-Bus battery has a cycle life of, for example, 3000 EFCs, the e-Bus could be operated for 13.7 years at 0.6 EFCs per day. With 1.1 EFCs per day, the operation time would be 7.5 years. The e-Boats, in turn, make fewer EFCs than the e-Buses. On median, e-Boats make 0.19 EFCs per day and 0.26 EFCs per day with activity. Thus, on average, the batteries in the six e-Boats complete more equivalent full cycles than the batteries in the 60 simulated e-Cars but fewer than the 52 e-Buses. If the EFCs per day with driving activity are calculated for the e-Boats, they are only 0.8% higher for one e-Boat that drives almost every day than if the EFCs were calculated for all days. The other extreme is an e-Boat that only drives every fourth day, which results in 0.026 EFCs per day, then 0.1 EFCs per day with driving activity.

Next to energy consumption and EFCs, other parameters are of relevance for the three modes of transport. For this purpose, Fig. 11 presents further boxplots of the three mobile applications. The boxplots of the mean SOCs of the means of transportation for the uncontrolled charging strategy are shown in Fig. 11 (a). The e-Cars show little spread; all have mean SOCs of 97.6–98.8%. In contrast, the mean SOCs of the e-Buses range from 72.8 to 88.7% SOC with a median of 81.2%. The median of the mean boot SOCs is 91.9%. Overall, the analyzed e-Bus

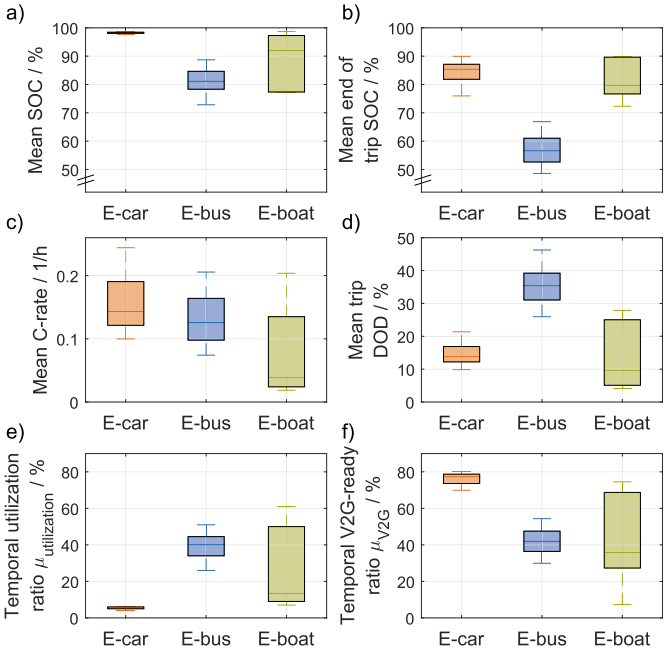

Fig. 11. E-Car (60, simulated), e-Bus (52, field data), and e-Boat (6, field data) boxplots of mean (a) and mean end of trip SOCs (b), mean C-rate (c), mean trip DOD (d), temporal utilization ratio (e) and temporal V2G-ready-ratio (f). The bus SOCs, C-rates, and DODs each refer to the useable capacity of the buses.

batteries are at the lowest average SOCs due to frequent and long trips, e-Car batteries are at the highest average SOCs, and e-Boat mean SOCs vary the most. For the selection of battery cells for vehicles, this means that in the case of uncontrolled charging, vehicle batteries should have comparatively low calendar degradation in high SOC ranges. This is especially relevant for private e-Cars.

Fig. 11 (b) shows the mean end-of-trip SOC of the three transportation means. For this parameter, the SOC is measured at the end of each trip, and then all these SOCs are averaged for each vehicle. The e-Cars have mean end-of-trip SOCs of 76–90% with a median of approximately 85%. The e-Buses, in contrast, end their trips with a mean SOC of 48–67% and a median of 56.5%. Last, the e-Boats have similar mean end-of-trip SOCs as the e-Cars of 72–90% (median 79.7%).

Diagram (c) of Fig. 11 shows the boxplots of the mean absolute C-rate of the e-Cars, e-Buses, and e-Boats. The average C-rates, meaning the current at which the batteries are discharged and charged normalized to the battery capacity in Ah, are between 0.018 and 0.244 1/h for all means of transport. E-Cars have the highest average C-rates at 0.10 to 0.244 1/h compared to e-Cars and e-Boats. The mean C-rates of the e-Buses range from 0.07 to 0.21 1/h, and that of the e-Boats is below 0.21 1/h. Here, the six e-Boats can be separated into two groups according to their battery capacity: Group 1 is Boat 1–3 and has battery capacities of 80–160 kWh. Group 2 is e-Boat 4–6 with battery capacities of 30–40 kWh (see Table A1). Group 1 then has very low C-rates of 0.024–0.042 1/h with an average of 0.033 1/h. Group 2, in contrast, shows an average C-rate of 0.119 1/h. Since the charging strategy influences the mean C-rate, we discuss this impact in more detail in section 4.4.

Subfigure (d) of Fig. 11 shows the mean DODs of a trip for the three modes, respectively, analogous to the SOC in (b). The mean trip DODs of the e-Cars range from 9.8 to 21.4%, with a median of 13.7%. In contrast, the mean trip DODs of the e-Buses are with 26–46% and a median of 35.3% higher than those of the e-Cars. Per trip, the mean DODs of the e-Boats range from 4.2 to 27.9% (d). Accordingly, the dataset includes e-Boats that complete only short trips and other e-Boats that consume more than a quarter of the batteries' energy per trip on average.

Last, the bottom two plots of Fig. 11 show the temporal utilization ratio $\mu_{utilization}$ (g) and the temporal V2G-ready ratio μ_{V2G} (h), presented in section 3.3. The temporal utilization ratio indicates the proportion of the time the vehicle is charged or discharged. The e-Cars in Fig. 11 (g) are used for charging or discharging only 4–6% of the time. This is in line with the statistics for private e-Cars in Germany, according to which they are used for trips only 3–4% of the time [16]. If the time spent charging the e-Cars is added, the 4–6% for $\mu_{utilization}$ is obtained. The e-Buses investigated in this study are used much more frequently compared to private e-Cars, showing values of 26–51% for $\mu_{utilization}$. Consequently, the e-Buses are used a quarter to half of the time either for trips or for charging the batteries. The e-Boat datasets show the greatest variation for the temporal utilization ratio. Thus, some e-Boats are used only 7% of the time, and other e-Boats are used 62% of the time, which is more than the most used e-Buses. However, when analyzing the utilization ratio of the e-Boats, it should be considered that the e-Boat data is available for three to nine months, mainly between May and November (see Fig. 4). Thus, actual utilization ratios of some rarely used e-Boats could be even lower over a whole year.

The temporal V2G-ready ratio μ_{V2G} in Fig. 11 (h) represents the fraction of time a vehicle is parked at the depot/at home/at the dock and thus plugged but not charging. For example, the analyzed private vehicles are at home 70–80% of the time and are not charged. Accordingly, the e-Cars could be used for V2G provision during this time. Consistent with Fig. 11 (g), e-Buses have less potential for V2G deployment. They are in the depot 30–54% of the time without being charged. However, e-Buses drive more predictable than private e-Cars, which means that e-Buses could also be used for V2G one-third to one-half of the time. Generally, e-Boats that are regularly docked in harbors could be used for V2G deployment. The e-Boats analyzed in this work differ significantly in μ_{V2G}, analogous to Fig. 11 (g). Some e-Boats are at the dock only 7% of the time without being charged. Other e-Boats, however, are idle up to 75% of the time. Consequently, the V2G potential of these means of transport depends strongly on the individual e-Boat.

Overall, the batteries in the means of transportation are stressed differently: E-Cars have relatively high mean SOCs with uncontrolled charging, are exposed to small DODs on average between charging events and undergo 0.1 to 0.2 cycles per day on average. For batteries in e-Cars, this means that calendar degradation is more relevant than cyclic degradation. Cells that exhibit accelerated calendar degradation at high SOCs appear less suitable for private e-Cars. In contrast, the average SOC of e-Buses is lower at around 80% when charging is uncontrolled. Furthermore, the e-Buses perform larger cycle depths between charging events and cope with 0.5–1 EFC daily. Accordingly, cyclic degradation appears more critical for the e-Buses than for the e-Cars studied in this work. Thus, cycle-stable battery cells should preferably be installed in e-Buses. The results for the e-Boats show the largest spreads, as there is a relatively large difference in driving patterns and usage among the six e-Boats. E-Boats should therefore be divided into subcategories when selecting battery cells. Generally, cycle depths between charging events are less than those of the e-Buses and may even be less than those of the e-Cars. The EFCs of the e-Boats are in the range of the e-Cars and, in some cases, below them. In view of the EFCs, mean SOCs, and C-rates, the use of typical e-Car batteries appears to make sense for most e-Boats. Regarding the temporal utilization ratio, especially private e-Cars are used rarely. This parameter is considerably higher for e-Buses. E-Boats also show a large spread here. The potential of vehicle utilization during idle times is demonstrated by the V2G-ready ratio: E-Cars and some of the e-Boats show the greatest potential, but the analyzed e-Buses are also parked in the depot for 30–54% of the time without being charged. Last, the estimated SOCs, C-rates, and DODs each refer to the useable capacity of the vehicles. By oversizing the battery and enabling specific voltage ranges, the actual battery SOCs might deviate from those shown, and the C-rates and trip DODs might decrease.

4.3. Comparison with stationary applications

Batteries are used in stationary applications in addition to the three mobile applications discussed in this work. For example, BSSs can be installed with PV systems to store PV surplus energy during the day and discharge the storage at night. This application leads to an increase in self-consumption (SCI). In addition, stationary BSSs can also be used to provide balancing power. In Central Europe, for example, there is a market for FCR in which BSSs can participate to balance frequency fluctuations in the grid. Another application of stationary BSSs is peak shaving (PS). In this application, which is often used at industrial sites, peak loads of the industrial customers are covered by the BSS, which reduces the power price of the electricity purchase. In a previous work, we evaluated the behavior of BSS in these three stationary applications concerning several battery parameters [45]. Fig. 12 compares three selected parameters of BSSs in mobile applications and values obtained for stationary applications. For the SCI boxplots, 74 simulated home storage profiles were evaluated for which the BSS was charged using the "greedy strategy," as is further explained in [45]. The FCR application shows the results of five BSSs with an LFP battery cell and modular inverter. Last, the PS boxplots show the distribution of 36 BSSs in the PS application that were divided into three clusters [45]. In [45], we have already shown the EFCs and mean DODs. For this work, we evaluated the power profiles of the stationary BSSs in terms of mean SOC and temporal utilization ratio.

Fig. 12 a) shows the number of EFCs the batteries complete daily in the six applications. Stationary BSSs in SCI and FCR perform a similar number of EFCs, averaging 0.77 and 0.7, respectively, as e-Buses with an average of 0.66. In contrast, e-Cars and e-Boats make fewer EFCs per day, with averages of 0.11 and 0.17, respectively, and stationary BSSs in PS application make the fewest EFCs, with an average of 0.07. Fig. 12 b) represents the mean SOC of the batteries in the six applications. The

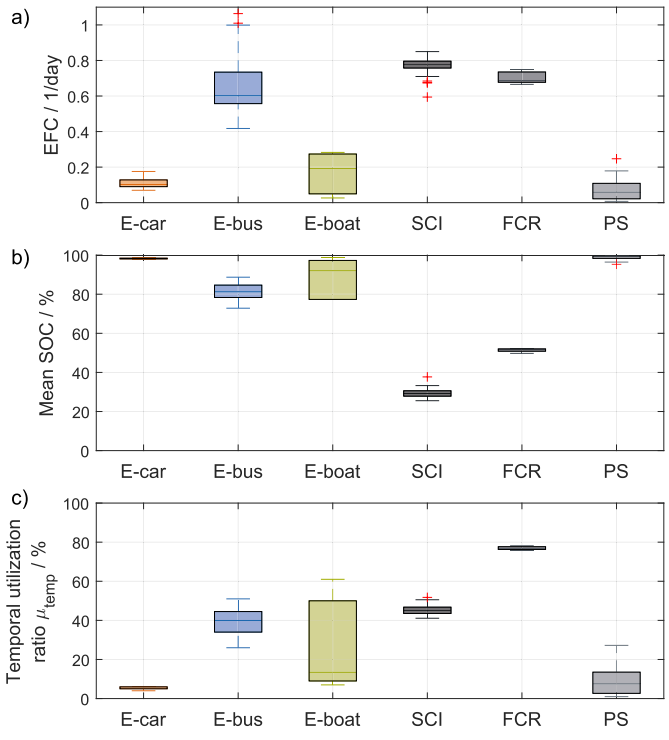

Fig. 12. Comparison of three parameters of mobile and stationary applications. SCI: self-consumption increase, FCR: frequency containment reserve, PS: peak-shaving.

mean SOC of BSSs in the PS application is in a similar range as the mean SOCs of the private e-Cars when they are charged uncontrolled immediately upon arrival. We show the influence of charging strategies on the mean SOC in section 4.4. In contrast, the BSSs in the FCR application have mean SOCs in the range of 49–53%. The mean SOCs of BSSs in SCI are the lowest, ranging from 25 to 37%. Fig. 12 c) shows the temporal utilization ratio as displayed in Fig. 11 f) for the transportation means. The temporal utilization of the stationary BSSs varies considerably: While FCR-BSS are used about 75–80% of the time, the ratio for PS-BSSs is, on average, only 9%. The utilization ratio of the SCI-BSS is between 40 and 50%. The utilization ratios of the mobile applications are all below 62%, which is below or equal to the FCR and SCI-BSS temporal utilization ratios.

In total, the parameters of the mobile and stationary applications show that, for example, in terms of equivalent full cycles and utilization ratios, e-Buses and SCI place a similar load on the battery. The impact on batteries in stationary PS-BSSs are similar to the load that e-Car batteries see in terms of the three parameters: Low number of cycles, high mean SOCs, and small usage times. Infrequently used e-Boat batteries experience similar loads as e-Cars and PS-BSS. As e-Buses, SCI BSS, and FCR BSS all post about a similar cycle load to a battery, those applications could aim for a similar type of cycle-stable battery. In contrast, e-Car, e-Boat, and PS BSS have low numbers of EFCs and could cope with a battery that does not provide high cycle stability. For the mean SOC, a similar interpretation is that calendar aging stability at high SOC values is relevant for e-Cars, e-Buses, e-Boats, and peak shaving, especially when the vehicles are charged uncontrolled. The temporal utilization ratio is of interest regarding V2G deployment. Thus, e-Cars could be combined with PS. However, a more detailed study is needed to determine whether e-Car use and PS demand coincide or at independent times of the day. The evaluation also suggests that discarded bus batteries designed for high cycles and medium utilization ratios could be used for SCI or FCR in second life. If, on the other hand, an increased number of cycles is already achieved in the first life of bus batteries, subsequent use in the PS application could make sense since this requires fewer cycles. Discarded e-Car batteries, optimized for high energy and power density rather than high cycle life, could also be used in stationary PS applications in second life.

4.4. Influence of charging strategies

This section investigates the charging strategy's impact on two parameters. For this purpose, the e-Cars, e-Buses, and e-Boats were simulated with the three charging strategies presented in section 3.2: uncontrolled charging, which was used for the results of the previous sections; charging with mean power; charging with a pause at 60% SOC. Fig. 13 shows the mean SOC (a) and mean C-rate (b) for the three strategies and the three modes of transportation. If the departure time is determined with the help of perfect foresight and charging is carried out with the mean power required, the mean SOC decreases because the vehicles are not parked for a long time at high SOCs. This strategy reduces the median of all mean SOCs by 3.4 (boats) to 8 (buses) percentage points. Above all, however, the mean C-rate is drastically reduced during charging. Thus, the C-rates of all vehicles are below 0.1 1/h. Especially the private e-Cars, with their long idle times between trips, show C-rates below 0.02 1/h with this strategy. In practice, this would correspond to charging rates of under 1.6 kW for the Tesla and under 1 kW for the Volkswagen. These low charging powers would lead to considerable efficiency losses in a wallbox designed for 11 kW [51], for example, which is why an economically optimal charging power probably lies between the mean power and the uncontrolled charging strategy power. The paused charging strategy, therefore, takes a different approach: After arrival, the vehicle is charged to a minimum SOC for spontaneous trips (60% in Fig. 13). The charging process is then paused and resumed shortly before the next journey. The effects of this strategy are shown in Fig. 13 on the right. Compared with the other two strategies, the paused charging strategy reduces mean SOCs. Thus, the e-Cars have mean SOCs around 90%, the e-Buses between 65 and 80%, and the e-Boats 76–97%. The generally still high SOCs, despite the break at 60% SOC, are because trips often end at higher SOCs (see Fig. 11 b). Note that active discharging down to 60% is not enforced in the simulations. The long idle time at high SOC increases the mean SOC despite applying the paused charging strategy. The mean charging rates of the vehicles in the paused strategy correspond to the rates of the uncontrolled strategy since charging is also performed at maximum charging power before and after the pause.

The break at 60% SOC is used as an example at this point to have

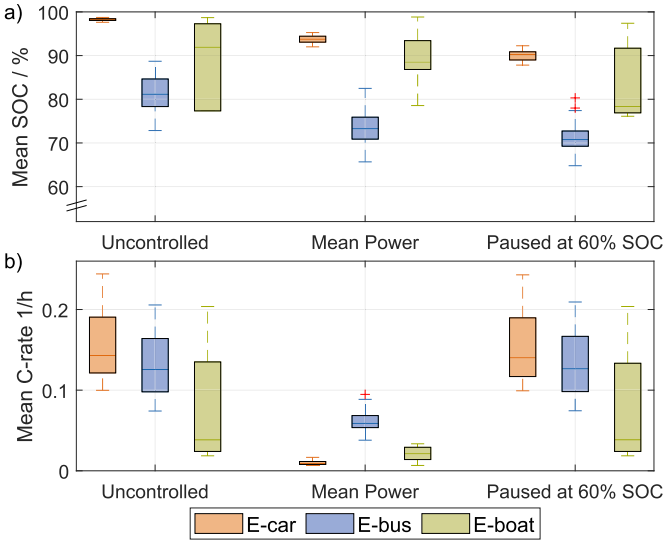

Fig. 13. Influence of charging strategies on mean SOC (a) and mean C-rate (b) for the three transportation means.

energy available for spontaneous departures. Generally, the setpoint value can vary between 0 and 100% SOC. A pause at 0% would mean that each vehicle is held at the arrival SOC and only charged shortly before departure. A delay at 100% SOC corresponds to the uncontrolled strategy. To show the impact of the pause SOC on the mean SOC, we have plotted the boxplots of all vehicle types for various pause thresholds in Fig. 14. If the pause SOC value is reduced from 100% progressively, the mean SOCs decrease. However, the potential of further reducing the pause SOC eventually saturates in all three vehicle categories. In the case of e-Cars, for example, reducing the pause SOC from 80 to 60% results in only a one percentage point reduction in the median SOC. The negligible impact of the threshold on cars is because cars often end their trips at relatively high SOCs (see Fig. 11 b) and subsequently hold the arrival SOC when the threshold SOC is below. As a result, the mean SOC remains high even at lower threshold SOCs. E-Boats and e-Buses, in contrast, saturate at lower pause SOC values. This is because their arrival SOCs are often lower than the arrival SOCs of the cars.

Overall, the evaluation shows the potential of charging strategies to reduce mean SOC and C-rate. For e-Cars, the results show that the mean SOC can be decreased by almost ten percentage points through paused charging. Due to the long idle times, this would certainly have a notable positive impact on calendar aging. The fact that the e-Cars often end their trips with a relatively high SOC means that a very low pause SOC does not significantly impact the mean SOC. Conversely, medium pause SOCs of 60% can also be selected without increasing the mean SOC significantly compared to a pause at 20%. For city e-Buses, the results imply that innovative charging strategies can reduce the mean SOC by over ten percentage points. E-Bus fleets often drive predictable routes. Furthermore, since trip DODs average below 50% (see Fig. 11), e-Buses could also be cycled in SOC ranges between 25 and 75%, thereby reducing calendar and cyclic aging of e-Bus batteries. The e-Boats can also reduce their mean SOC and C-rate depending on their driving style. Specifically, infrequently used e-Boats with small trip DODs could be cycled like the e-Buses by smart charging in medium SOC ranges. The same applies to frequent ferries as long as the route is foreseeable. Other charging strategies not simulated in this work could charge the vehicles to the SOC needed for the next day instead of 100%. This would further reduce the mean SOC but also require forecasting the required energy, which is more feasible for city buses than for private cars. In addition to these unidirectional strategies, bidirectional strategies could be developed to enable the deployment of V2G. Those strategies could build on the paused strategy, as the vehicle is charged to a minimum SOC for spontaneous trips and then paused until shortly before departure. During this pause, the vehicle could provide V2G services.

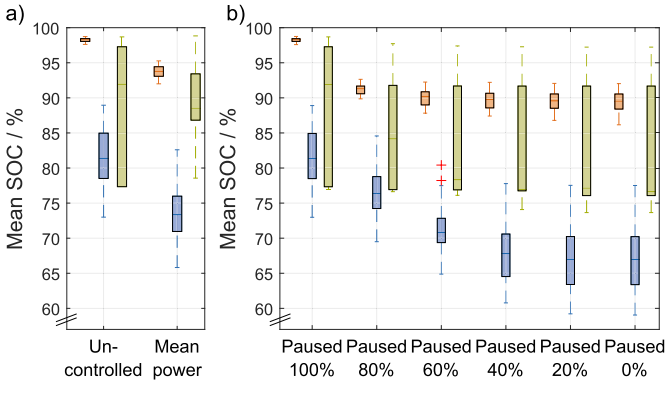

Fig. 14. Charging strategy sensitivity analysis: a) Mean vehicle SOCs for the uncontrolled and the mean power charging strategy. b) Mean vehicle SOCs for the paused charging strategy in dependence on the pause SOC. In the e-Bus simulations, a time resolution of 60s is chosen.

5. Conclusion and outlook

This work evaluated the impact of the operation of three electrified transportation modes on batteries using battery-relevant parameters. Simulated data from 60 e-Cars and field data from 82 e-Buses and six e-Boats were used. The data was pre-processed, analyzed, and filtered in the first step. Thus, 30 of the 82 e-Buses were filtered out due to insufficient data length or quality. For the analysis of the transportation modes, the simulation tool *SimSES* developed for stationary BSS was extended to mobile BSS by using vehicle availability as a binary value. The presentation of the *SimSES* extension in Section 3.2 answers RQ1, how various transportation modes can be simulated with an open-source storage simulation tool.

As the first part of the evaluation, we analyzed the energy consumption of the e-Cars and e-Buses. Here, we found that the simulated e-Cars consume between 0.18 and 0.29 kWh/km, while the consumption of the e-Buses is between 0.9 and 1.6 kWh/km (RQ 2). For the e-Buses, consumption increases with larger e-Bus batteries, probably due to the larger and heavier vehicles. However, the scatter within the e-Bus categories showed that other influencing factors could lead to higher or lower consumption. One of these influencing factors is the ambient temperature. If trips occurred around 20–22 °C, the e-Buses showed an average energy consumption of approximately 1 kWh/km. At higher and lower temperatures, consumption increased by about 2–3% per 1 °C symmetrically. At temperatures below 10 °C, the e-Bus models showed varying behavior. For e-Bus models with electric heating, consumption below 8 °C increased as the temperature dropped. For e-Bus models with additional conventional heating systems, consumption below 8 °C decreased again because the battery was not utilized for heating.

Next, we evaluated the stress on the vehicle batteries regarding various battery-relevant parameters (RQ 3). This analysis showed that e-Cars make between 0.07 and 0.18 EFCs per day, while e-Buses make 0.4 to more than 1 EFC per day. The six e-Boats analyzed make 0.026 to 0.28 EFCs per day. If only days with driving activity are considered, the EFCs increase by 50%–70% for e-Cars, up to 23% for e-Buses, and up to a factor of four for e-Boats. Regarding other parameters, the batteries in the means of transport are also differently stressed: Cars are often in high SOC ranges of 98% on average with uncontrolled charging and experience relatively small cycle depths of 10–22% during trips. E-Buses, in contrast, have mean SOCs of around 80% and experience larger mean trip cycle depths of up to 46%. The six e-Boats differ more in size and driving characteristics than the other two modes of transportation. The mean SOCs of the e-Boats range from 76 to 98.7%, and the trip cycle depths are between 4 and 28%. Accordingly, for the detailed characterization of specific e-Boats, they could be divided into subcategories, such as ferries and recreational boats. Furthermore, the analysis of the temporal utilization ratio and the temporal V2G-ready ratio showed that e-Cars are parked and idle for 70–80% of the time. During these times, e-Cars could provide V2G services. In contrast, the temporal V2G potential of e-Buses is lower at 30–54%. However, due to the predictability of departure times of city e-Buses, they could also provide V2G services well. E-Boats again showed more significant differences between recreational boats that are idle for extended periods and ferries that move a lot.

The comparison with stationary applications showed that the three parameters evaluated can have similarities with mobile applications (RQ 4). E-Buses and stationary home BSS (SCI) stress the batteries similarly concerning EFCs and utilization ratios, although the mean SOCs differ. Stationary BSSs in PS application and e-Cars result in equally low numbers of EFCs and low utilization ratios. In addition, the mean SOCs are similar in these two applications. Next, our sensitivity analysis of charging strategies showed that the mean SOCs of vehicles could be reduced by 8–13.8% points through smart charging strategies like paused charging at 60% SOC (RQ 5). In contrast, charging at the lowest possible power reduces the C-rate that vehicle batteries face to below 0.1 1/h for all vehicle types. These evaluations demonstrate the

potential of smart charging strategies to reduce battery aging stress factors.

Moreover, as part of this study, an open data repository is provided for both e-Bus and e-Boat data [52]. On the e-Bus side, we have uploaded the raw data and simulation results of the 52 used e-Buses. On the side of the e-Boats, the raw data and simulation results of the six e-Boats have been uploaded. Moreover, the e-Car results and the parameters determined are part of the open data repository. Others are encouraged to use the data in research and industry for their simulations and evaluations.

More in-depth analyses are possible building on our work. The six e-Boats represent only a small excerpt from the entire market of e-Boats. Due to the mix of ferries and private e-Boats, the results already show a range of the driving behavior of the e-Boats. Moreover, the e-Bus data and their consumption could be evaluated further, for example, based on speeds driven or weather conditions. If the vehicles were measured with a 1-s resolution, statements could also be made about the exact DOD, including recuperation, and not just about trip DODs. In addition, the work could be expanded to include other mobile applications. In this work, we have presented parameters that quantify the load on vehicle batteries. These parameters are partly stress factors that influence the degradation of batteries. Building on our work, aging models of specific battery cells could be used to quantify calendar and cyclic aging. Furthermore, the results can be used to explicitly optimize battery cells with respect to the load in the various transportation modes. In addition, all vehicle types have idle times in the depot or at home, during which the vehicles are not used. At these times, the vehicles could be used for V2G generation to utilize the resources used for battery production to the greatest extent possible. Finally, the evaluations can be used and extended to assess the second-life suitability of batteries from mobile applications for stationary applications.

CRediT authorship contribution statement

Benedikt Tepe: Conceptualization, Methodology, Software, Formal analysis, Investigation, Writing – original draft, Visualization. **Sammy Jablonski:** Conceptualization, Methodology, Writing – original draft, Visualization. **Holger Hesse:** Conceptualization, Writing – review & editing, Supervision. **Andreas Jossen:** Resources, Writing – review & editing, Supervision.

Declaration of generative AI and AI-assisted technologies in the writing process

During the preparation of this work the authors used Grammarly and DeepL in order to improve the syntax and grammar of the text. After using these services, the authors reviewed and edited the content as needed and take full responsibility for the content kof the publication.

Declaration of competing interest

The authors declare that they have no known competing financial interests or personal relationships that could have appeared to influence the work reported in this paper.

Data availability

In agreement with Hochbahn Hamburg and Torqeedo, we have published the data on which this publication is based, together with our simulation results, as open data [52]. The link in the reference leads to the media and publications repository of the Technical University of Munich. Moreover, the extended open-source version of *SimSES* can also be found in [52]. Recent versions of *SimSES* can be found in [53].

Acknowledgment

We thank Hamburger Hochbahn AG, Torqeedo, and DIW Berlin for their cooperation and data sharing, without which this work would not have been possible. This work was financially supported by the German Federal Ministry of Education and Research (BMBF) within the SimBAS project (Grant No. 03XP0338A), which is managed by Project Management Jülich. The responsibility for this publication rests with the authors.

Appendix

Raw data details

Table A1 shows detailed vehicle information about the three means of transportation

Preprocessing – Creation of binary profiles

Table A1
Vehicle information about the e-Cars, e-Buses, and e-Boats. The second column shows the number of records of the respective vehicle type after filtering. The last column gives additional information (e-Car: Driver type, e-Bus: SOC resolution, e-Boats: weight).

Data	#	Battery Capacity	Max. Battery Power	Charging Power	Vehicle info	Other info
Car A_F	10	45 kWh	93 kW	11 kW	VW ID.3	Driver type: Fulltime
Car A_P	10	45 kWh	93 kW	11 kW	VW ID.3	Parttime
Car A_L	10	45 kWh	93 kW	11 kW	VW ID.3	Leisure/Freetime
Car B_F	10	79.5 kWh	358 kW	11 kW	Tesla Model 3	Fulltime
Car B_P	10	79.5 kWh	358 kW	11 kW	Tesla Model 3	Parttime
Car B_L	10	79.5 kWh	358 kW	11 kW	Tesla Model 3	Leisure/Freetime
Bus A	9	190 kWh	350 kW	150 kW	Evobus NMC	SOC res. 0.5%
Bus B	6	240 kWh	350 kW	150 kW	Solaris NMC	0.4%
Bus C	5	291 kWh	350 kW	80 kW	Evobus LMP	0.5%
Bus D	6	309 kWh	350 kW	150 kW	Evobus NMC	0.5%
Bus E	3	316 kWh	350 kW	150 kW	Solaris NMC	0.01%
Bus F	23	397 kWh	350 kW	80 kW	Evobus LMP	0.5%
Boat 1	1	160 kWh	320 kW	8.93 kW	–	Weight: 7.5t
Boat 2	1	120 kWh	320 kW	7.82 kW	–	37t
Boat 3	1	80 kWh	160 kW	23.53 kW	–	18t
Boat 4	1	30 kWh	80 kW	8.73 kW	–	2t
Boat 5	1	40 kWh	80 kW	2.66 kW	–	1.5t
Boat 6	1	40 kWh	80 kW	5.58 kW	–	1t

For the creation of the e-Bus binary profiles, it is assumed that an e-Bus is connected to the grid if the SOC is greater than or equal to 99% or if the SOC increases, meaning the vehicle is charged (equation (6.1)). However, positive SOC deltas can also occur during journeys since the e-Bus can recuperate during braking while driving. In addition, there can be fluctuations in the SOC estimator so that the SOC increases slightly for a short time during trips. For this reason, we introduce as an additional condition that a contiguous depot time for charging the e-Bus must be at least 10 min long. Consequently, all binary values in the profile that are not part of a charging phase lasting at least 10 min are counted as journey times and set to zero. Finally, the binary profile is saved as CSV, together with the time stamp.

$$b(t) = \begin{cases} 1, SOC(t) \geq 99\% \vee \Delta SOC(t) > 0 \\ 0, otherwise \end{cases} \tag{6.1}$$

With: $\Delta SOC(t) = SOC(t) - SOC(t-1)$.

In addition, analogous to the e-Buses, binary profiles of the e-Boats are created, which indicate whether the e-Boat is connected to the electricity grid. Since SOC and power data are available for the e-Boats, the binary profiles are formed according to equation (6.2). First, analogous to the e-Buses, the binary value is set to one when the SOC is at least 99%. Furthermore, the e-Boat is defined as connected to the electricity grid if the power is positive. As for the e-Buses, we further use the condition that a contiguous grid connection time must be at least 10 min long. This way, short periods during driving with positive power values are not counted as “connected to the grid".

$$b(t) = \begin{cases} 1, SOC(t) \geq 99\% \vee P(t) > 0 \\ 0, otherwise \end{cases} \tag{6.2}$$

Lithium-ion battery specifications

Table A2
Lithium-ion battery cell specifications [42,54].

Manufacturer	Sanyo
Model	UR18650E
Capacity (minimum/typical)	2.05 Ah/2.15 Ah
Allowed voltage range	2.5 V–4.2 V
Proposed voltage range	3.0 V–4.1 V
Cathode active material	$Li(NiMnCo)O_2$
Anode active material	Graphite
Electrolyte material	1 M LiPF6 in an EC/EMC (1:1) solvent mixture

Table A2 shows detailed vehicle information about the three means of transportation.

E-Bus energy consumption – temperature analysis

Fig. A1 depicts the boxplot diagram of the energy consumption of all buses depending on the ambient temperature, including outliers. In Fig. 8, the data is plotted without outliers. Moreover, Fig. A2 shows the energy consumption of all bus types separately depending on the ambient temperature.

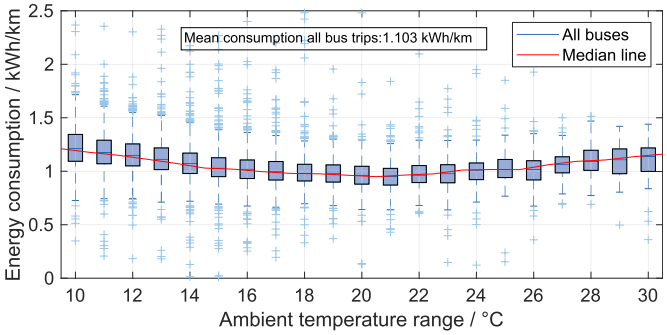

Fig. A1. Boxplot diagram of the energy consumption depending on the ambient temperature for all e-busses of all categories. Outliers are shown in blue to not distract from the general trend.

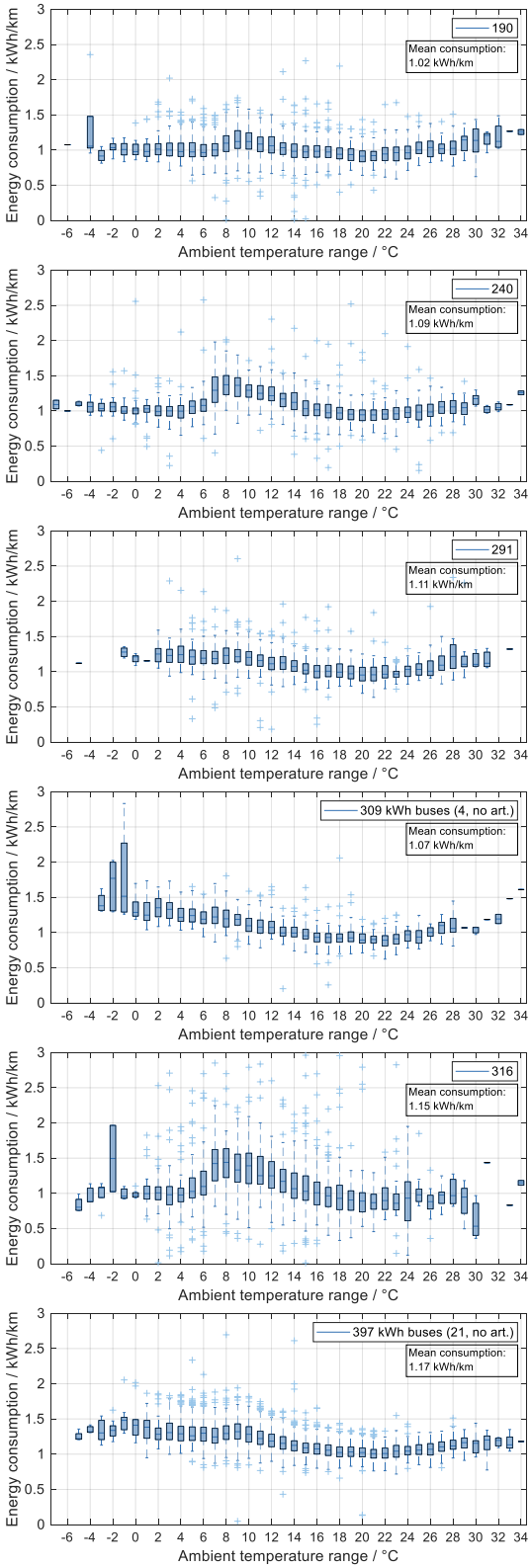

Fig. A2. Bus temperature analysis detailed boxplots of all types of e-Buses. The number in the legend indicates the e-Bus battery capacities. Two articulated buses in the 309-kWh category and two articulated buses in the 397-kWh category are excluded.

References

[1] Li M, Lu J, Chen Z, Amine K. 30 Years of lithium-ion batteries. Adv Mater 2018;30 (33):1800561. https://doi.org/10.1002/adma.201800561.

[2] Bibra EM, Connelly E, Dhir S, Drtil M, Henriot P, Hwang I, et al. Global EV outlook 2022:securing supplies for an electric future. International Energy Agency (IEA); 2022.

[3] Bloomberg New Energy Finance. Electric buses in Cities: driving towards cleaner air and Lower CO2. Bloomberg Finance LP; 2018.

[4] Sameer J. Electric boat market size worth $11.35 billion, globally, by 2028 at 13.7% CAGR: the insight partners. GlobeNewswire 2022. 8 November 2022; Available from: https://www.globenewswire.com/en/news-release/2022/11/08/2551096/0/en/Electric-Boat-Market-Size-Worth-11-35-Billion-Globally-by-2028-at-13-7-CAGR-The-Insight-Partners.html.

[5] Randall C. Germany funds 472 new electric buses for Hamburg 2022, 1 April 2022; Available from: https://www.electrive.com/2022/04/01/germany-funds-472-new-electric-buses-for-hamburg/.

[6] Möller M, Kucevic D, Collath N, Parlikar A, Dotzauer P. Tepe B et al. SimSES: a holistic simulation framework for modeling and analyzing stationary energy storage systems. J Energy Storage 2022;49:103743. https://doi.org/10.1016/j.est.2021.103743.

[7] Al-Ogaili AS, Tengku Hashim TJ, Rahmat NA, Ramasamy AK, Marsadek MB, Faisal M, et al. Review on scheduling, clustering, and forecasting strategies for controlling electric vehicle charging: challenges and recommendations. IEEE Access 2019;7:128353–71. https://doi.org/10.1109/ACCESS.2019.2939595.

[8] Kim J, Oh J, Lee H. Review on battery thermal management system for electric vehicles. Appl Therm Eng 2019;149:192–212. https://doi.org/10.1016/j.applthermaleng.2018.12.020.

[9] De Cauwer C, Maarten M, Heyvaert S, Coosemans T, van Mierlo J. Electric vehicle use and energy consumption based on realworld electric vehicle fleet trip and charge data and its impact on existing EV research models. WE! 2015;7(3):436–46. https://doi.org/10.3390/wevj7030436.

[10] Hao X, Wang H, Lin Z, Ouyang M. Seasonal effects on electric vehicle energy consumption and driving range: a case study on personal, taxi, and ridesharing vehicles. J Clean Prod 2020;249:119403. https://doi.org/10.1016/j.jclepro.2019.119403.

[11] Chen X, Li K, Zhang H, Yuan Q, Ye Q. Identifying and recognizing usage pattern of electric vehicles using GPS and on-board diagnostics data. In: Zhang G, editor. International conference on transportation and development 2020. Reston, VA: American Society of Civil Engineers; 2020. p. 85–97. https://doi.org/10.1061/9780784483138.008.

[12] Tansini A, Di Pierro G, Fontaras G, Gil-Sayas S, Komnos D, Currò D. Battery electric vehicles energy consumption breakdown from on-road trips. SAE Int. J. Adv. & Curr. Prac. in Mobility 2023;5(3):977–87. https://doi.org/10.4271/2022-37-0009.

[13] Zou Y, Wei S, Sun F, Hu X, Shiao Y. Large-scale deployment of electric taxis in Beijing: A real-world analysis. Energy 2016;100:25–39. https://doi.org/10.1016/j.energy.2016.01.062.

[14] Weldon P, Morrissey P, Brady J, O'Mahony M. An investigation into usage patterns of electric vehicles in Ireland. Transport Res Transport Environ 2016;43:207–25. https://doi.org/10.1016/j.trd.2015.12.013.

[15] Zhang J, Wang Z, Liu P, Zhang Z. Energy consumption analysis and prediction of electric vehicles based on real-world driving data. Appl Energy 2020;275:115408. https://doi.org/10.1016/j.apenergy.2020.115408.

[16] Nobis C, Kuhnimhof T. Mobilität in Deutschland – MiD. Ergebnisbericht.: Studie von infas, DLR, IVT und infas 360 im Auftrag des Bundesministers für Verkehr und digitale infrastruktur (FE-Nr. 70.904/15). Bonn, Berlin. 2018.

[17] Follmer R, Gruschwitz D. Mobility in Germany – short report: Edition 4.0 of the study by infas, DLR, IVT and infas 360 on behalf of the Federal Ministry of transport and digital infrastructure (BMVI) (FE no. 70.904/15). Bonn, Berlin. 2019.

[18] Gaete-Morales C, Kramer H, Schill W-P, Zerrahn A. An open tool for creating battery-electric vehicle time series from empirical data, emobpy. Sci Data 2021;8(1):152. https://doi.org/10.1038/s41597-021-00932-9.

[19] Manzolli JA, Trovão JP, Antunes CH. A review of electric bus vehicles research topics – methods and trends. Renew Sustain Energy Rev 2022;159:112211. https://doi.org/10.1016/j.rser.2022.112211.

[20] Rogge M, Wollny S, Sauer DU. Fast charging battery buses for the electrification of urban public transport—a feasibility study focusing on charging infrastructure and energy storage requirements. Energies 2015;8(5):4587–606. https://doi.org/10.3390/en8054587.

[21] Sinhuber P, Rohlfs W, Sauer DU. Study on power and energy demand for sizing the energy storage systems for electrified local public transport buses. In: 2012 IEEE vehicle power and propulsion conference. IEEE; 2012. p. 315–20. https://doi.org/10.1109/VPPC.2012.6422680.

[22] Gallet M, Massier T, Hamacher T. Estimation of the energy demand of electric buses based on real-world data for large-scale public transport networks. Appl Energy 2018;230:344–56. https://doi.org/10.1016/j.apenergy.2018.08.086.

[23] Gao Z, Lin Z, LaClair TJ, Liu C, Li J-M, Birky AK, et al. Battery capacity and recharging needs for electric buses in city transit service. Energy 2017;122:588–600. https://doi.org/10.1016/j.energy.2017.01.101.

[24] Wang S, Lu C, Liu C, Zhou Y, Bi J, Zhao X. Understanding the energy consumption of battery electric buses in urban public transport systems. Sustainability 2020;12(23):10007. https://doi.org/10.3390/su122310007.

[25] Du J, Zhang X, Wang T, Song Z, Yang X, Wang H, et al. Battery degradation minimization oriented energy management strategy for plug-in hybrid electric bus with multi-energy storage system. Energy 2018;165:153–63. https://doi.org/10.1016/j.energy.2018.09.084.

[26] Zhang L, Wang S, Qu X. Optimal electric bus fleet scheduling considering battery degradation and non-linear charging profile. Transport Res E Logist Transport Rev 2021;154:102445. https://doi.org/10.1016/j.tre.2021.102445.

[27] Manzolli JA, Trovão JPF, Henggeler Antunes C. Electric bus coordinated charging strategy considering V2G and battery degradation. Energy 2022;254:124252. https://doi.org/10.1016/j.energy.2022.124252.

[28] Spagnolo GS, Papalillo D, Martocchia A, Makary G. Solar-electric boat. JTTs 2012;2(2):144–9. https://doi.org/10.4236/jtts.2012.22015.

[29] Kabir SL, Alam I, Khan MR, Hossain MS, Rahman KS, Amin N. Solar powered ferry boat for the rural area of Bangladesh. In: 2016 International conference on advances in electrical, electronic and systems engineering (ICAEES). IEEE; 2016. p. 38–42. https://doi.org/10.1109/ICAEES.2016.7888005.

[30] Soleymani M, Yoosofi A, Kandi -DM. Sizing and energy management of a medium hybrid electric boat. J Mar Sci Technol 2015;20(4):739–51. https://doi.org/10.1007/s00773-015-0327-0.

[31] Tepe B, Figgener J, Englberger S, Sauer DU, Jossen A, Hesse H. Optimal pool composition of commercial electric vehicles in V2G fleet operation of various electricity markets. Appl Energy 2022;308:118351. https://doi.org/10.1016/j.apenergy.2021.118351.

[32] Lacey G, Putrus G, Bentley E. Smart EV charging schedules: supporting the grid and protecting battery life. IET Electr Syst Transp 2017;7(1):84–91. https://doi.org/10.1049/iet-est.2016.0032.

[33] Rücker F, Bremer I, Sauer DU. Development and analysis of a charging algorithm for electric vehicle fleets extending battery lifetime. In: 2016 IEEE transportation electrification Conference, Asia-Pacific (ITEC Asia-Pacific); 2016. p. 29–33. https://doi.org/10.1109/ITEC-AP.2016.7512917.

[34] Hu X, Xu Le, Lin X, Pecht M. Battery lifetime prognostics. Joule 2020;4(2):310–46. https://doi.org/10.1016/j.joule.2019.11.018.

[35] Schuller A, Dietz B, Flath CM, Weinhardt C. Charging strategies for battery electric vehicles: economic benchmark and V2G potential. IEEE Trans Power Syst 2014;29(5):2014–22. https://doi.org/10.1109/TPWRS.2014.2301024.

[36] Tuchnitz F, Ebell N, Schlund J, Pruckner M. Development and evaluation of a smart charging strategy for an electric vehicle fleet based on reinforcement learning. Appl Energy 2021;285:116382. https://doi.org/10.1016/j.apenergy.2020.116382.

[37] Abdullah Al-Karakchi AA, Putrus G, Das R. Smart EV charging profiles to extend battery life. In: 2017 52nd International universities power cngineering conference (UPEC). IEEE; 2017. p. 1–4. https://doi.org/10.1109/UPEC.2017.8231961.

[38] Chen J, Huang X, Tian S, Cao Y, Huang B, Luo X, et al. Electric vehicle charging schedule considering user's charging selection from economics. IET Gener, Transm Distrib 2019;13(15):3388–96. https://doi.org/10.1049/iet-gtd.2019.0154.

[39] Houbbadi A, Trigui R, Pelissier S, Redondo-Iglesias E, Bouton T. Optimal scheduling to manage an electric bus fleet overnight charging. Energies 2019;12(14):2727. https://doi.org/10.3390/en12142727.

[40] Shaukat N, Khan B, Ali SM, Mehmood CA, Khan J, Farid U, et al. A survey on electric vehicle transportation within smart grid system. Renew Sustain Energy Rev 2018;81:1329–49. https://doi.org/10.1016/j.rser.2017.05.092.

[41] Gschwendtner C, Sinsel SR, Stephan A. Vehicle-to-X (V2X) implementation: an overview of predominate trial configurations and technical, social and regulatory challenges. Renew Sustain Energy Rev 2021;145:110977. https://doi.org/10.1016/j.rser.2021.110977.

[42] Schmalstieg J, Käbitz S, Ecker M, Sauer DU. A holistic aging model for Li(NiMnCo)O2 based 18650 lithium-ion batteries. J Power Sources 2014;257:325–34. https://doi.org/10.1016/j.jpowsour.2014.02.012.

[43] Naumann M, Schimpe M, Keil P, Hesse H, Jossen A. Analysis and modeling of calendar aging of a commercial LiFePO4/graphite cell. J Energy Storage 2018;17:153–69. https://doi.org/10.1016/j.est.2018.01.019.

[44] Naumann M, Spingler FB, Jossen A. Analysis and modeling of cycle aging of a commercial LiFePO4/graphite cell. J Power Sources 2020;451:227666. https://doi.org/10.1016/j.jpowsour.2019.227666.

[45] Kucevic D, Tepe B, Englberger S, Parlikar A, Mühlbauer M, Bohlen O, et al. Standard battery energy storage system profiles: analysis of various applications for stationary energy storage systems using a holistic simulation framework. J Energy Storage 2020;28:101077. https://doi.org/10.1016/j.est.2019.101077.

[46] Dataforce. Leading models of battery-electric passenger cars and light commercial vehicles by new registrations in the European Union in 2021. Statista. [July 18, 2023]; Available from: https://www.statista.com/statistics/1301916/bev-leading-models-europe/.

[47] Kraftfahrt-Bundesamt. Entwicklung der Fahrleistungen nach Fahrzeugarten (engl. German Federal Motor Transport Authority - development of mileage by vehicle type). . [July 18, 2023]; Available from: https://www.kba.de/DE/Statistik/Kraftverkehr/VerkehrKilometer/vk_inlaenderfahrleistung/2021/verkehr_in_kilometern_kurzbericht_pdf.pdf?__blob=publicationFile&v=2.

[48] Notton G, Lazarov V, Stoyanov L. Optimal sizing of a grid-connected PV system for various PV module technologies and inclinations, inverter efficiency characteristics and locations. Renew Energy 2010;35(2):541–54. https://doi.org/10.1016/j.renene.2009.07.013.

[49] Collath N, Tepe B, Englberger S, Jossen A, Hesse H. Aging aware operation of lithium-ion battery energy storage systems: a review. J Energy Storage 2022;55:105634. https://doi.org/10.1016/j.est.2022.105634.

[50] You S, Rasmussen CN. Generic modelling framework for economic analysis of battery systems. In: IET conference on renewable power generation (RPG 2011). IET; 2011. p. 122. https://doi.org/10.1049/cp.2011.0147.

[51] Biroon RA, Abdollahi Z, Hadidi R. Inverter's nonlinear efficiency and demand-side management challenges. IEEE Power Energy Mag 2021;8(1):49–54. https://doi.org/10.1109/MPEL.2020.3047527.

[52] Tepe B, Jablonski S, Hesse H, Jossen A. Lithium-Ion Battery Utilization in various Modes of e-Transportation - Dataset. Available from: https://mediatum.ub.tum.de/1709192.

[53] Chair of Electrical Energy Storage Technology, Technical University of Munich. Simulation of stationary energy storage systems (SimSES). https://gitlab.lrz.de/open-ees-ses/simses.

[54] Ecker M, Nieto N, Käbitz S, Schmalstieg J, Blanke H, Warnecke A, et al. Calendar and cycle life study of Li(NiMnCo)O2-based 18650 lithium-ion batteries. J Power Sources 2014;248:839–51. https://doi.org/10.1016/j.jpowsour.2013.09.143.